Engineered live bacteria suppress *Pseudomonas aeruginosa* infection in mouse lung and dissolve endotracheal-tube biofilms

Rocco Mazzolini[1,2,11], Irene Rodríguez-Arce[1,3,11], Laia Fernández-Barat [4,5], Carlos Piñero-Lambea [1,2], Victoria Garrido [1,3], Agustín Rebollada-Merino [6,7], Anna Motos[4,5], Antoni Torres [4,5], Maria Jesús Grilló [3], Luis Serrano [1,8,9] ✉ & Maria Lluch-Senar [1,2,10] ✉

Engineered live bacteria could provide a new modality for treating lung infections, a major cause of mortality worldwide. In the present study, we engineered a genome-reduced human lung bacterium, *Mycoplasma pneumoniae*, to treat ventilator-associated pneumonia, a disease with high hospital mortality when associated with *Pseudomonas aeruginosa* biofilms. After validating the biosafety of an attenuated *M. pneumoniae* chassis in mice, we introduced four transgenes into the chromosome by transposition to implement bactericidal and biofilm degradation activities. We show that this engineered strain has high efficacy against an acute *P. aeruginosa* lung infection in a mouse model. In addition, we demonstrated that the engineered strain could dissolve biofilms formed in endotracheal tubes of patients with ventilator-associated pneumonia and be combined with antibiotics targeting the peptidoglycan layer to increase efficacy against Gram-positive and Gram-negative bacteria. We expect our *M. pneumoniae*-engineered strain to be able to treat biofilm-associated infections in the respiratory tract.

Respiratory diseases are among the top ten causes of death worldwide. Efforts to develop new therapeutics against respiratory tract infections are growing, especially given the mounting concern about antibiotic-resistant bacteria and the paucity of new antibiotics[1]. Moreover, antibiotic therapies eliminate beneficial lung microbes and can lead to the persistence of pathogenic, resistant strains[2]. Approximately 65–80% of human infections are associated with biofilms[3–6]. They are especially frequent in pulmonary chronic diseases[7,8], including cystic fibrosis (CF)[9], chronic obstructive pulmonary disease[8] and non-CF bronchiectasis, as well as in acute airway infections, such as ventilator-associated tracheobronchitis (VAT) and ventilator-associated pneumonia (VAP)[10,11]. Biofilms are an ancestral bacterial survival strategy against environmental stress that consists of complex and dynamic structures formed by aggregates of microorganisms embedded in a polymeric matrix, which confers tolerance to antimicrobials[12,13] and allows them to evade host defense

[1]Centre for Genomic Regulation, Barcelona Institute of Science and Technology, Barcelona, Spain. [2]Pulmobiotics Ltd, Barcelona, Spain. [3]Institute of Agrobiotechnology, CSIC-Navarra Government, Navarra, Spain. [4]Cellex Laboratory, CibeRes, Institut d'Investigacions Biomèdiques August Pi i Sunyer, University of Barcelona, Barcelona, Spain. [5]Department of Pneumology, Thorax Institute, Hospital Clinic of Barcelona, SpainICREA, Barcelona, Spain. [6]VISAVET Health Surveillance Centre, Complutense University of Madrid, Madrid, Spain. [7]Department of Internal Medicine and Animal Surgery, Faculty of Veterinary Medicine, Complutense University of Madrid, Madrid, Spain. [8]Universitat Pompeu Fabra, Barcelona, Spain. [9]ICREA, Barcelona, Spain. [10]Basic Sciences Department, Faculty of Medicine and Health Sciences, Universitat Internacional de Catalunya, Sant Cugat del Vallès, Spain. [11]These authors contributed equally: Rocco Mazzolini, Irene Rodríguez-Arce. ✉e-mail: luis.serrano@crg.eu; maria.lluch@pulmobio.com

Table 1 | Dose–response of WT or CV2 _M. pneumoniae_ strain lung infection

	WT				CV2			
Inoculation dose (c.f.u. per mouse)	10^4	10^6	10^7	10^8	10^4	10^6	10^7	10^8
_n_=mice infected/total	1/7	7/7	5/5	7/7	0/7	5/7	6/6	5/5
$\log_{10}$(c.f.u. per lung) (mean±s.d.)	0.9±0.2	3.3±0.9	3.6±0.9	6.4±0.7	0.8±0.07	2.4±1.1	4.0±0.7	5.9±0.7

CD1 mice (_n_=5–7) were inoculated i.t. with increasing doses of WT or CV2 _M. pneumoniae_. At 4 d.p.i., the ratio of infected mice and the $\log_{10}$(c.f.u. per lung) ($\log_{10}$(mean±s.d.)) were determined.

mechanisms[14]. Thus, biofilms can cause recurrent, device-associated chronic infections. As a result, the effective minimum bactericidal concentrations of antibiotics for biofilm eradication in vivo are relatively high and can cause adverse effects, such as renal and/or hepatic injury[15]. Moreover, many of the lung pathogenic bacterial strains are resistant to antibiotics.

Biofilm formation is especially problematic with the use of endotracheal tubes (ETTs) in patients who require invasive mechanical ventilation (MV) in intensive care units (ICUs). VAT and VAP are estimated to occur in 9–27% of all patients receiving MV[16]. For patients with severe acute respiratory syndrome coronavirus 2 (SARS-CoV-2) who receive MV, the incidence rates of VAP/VAT are higher than usual and exceed 50% overall[17]. Moreover, the mortality rate in VAP patients with COVID-19 was higher than in those with influenza or without viral infection[18,19] and even higher when associated with _P. aeruginosa_ biofilms[20,21]. Until now, most interventions aimed at reducing lung biofilms, including aerosolized antibiotics, have failed or require further investigation[22].

Engineered bacteria that are genetically modified to treat diseases—which are classified as live biotherapeutic products—could offer effective therapeutic formulations with fewer adverse effects[23–34]. Most bacterial vectors have been designed to treat gut diseases, with a few targeting diseases affecting other organs. Examples include an engineered strain of _Lactobacillus reuteri_ that decreases high blood levels of phenylalanine in a homozygous _PAHenu2_ (phenylketonuria) mouse model[25] and an engineered strain of _Lactobacillus_ spp. or _Saccharomyces cerevisiae_ designed to immunize against HIV in the gut[27] and the cervicovaginal mucosa[35,36]. However, no bacterial chassis has so far been described for the treatment of lung diseases[37].

The site of action of a bacterial therapeutic affects the choice of species[38]. Ideally, the selected bacterium should be naturally present in the organ to be treated, to ensure its survival and limit spreading to other organs. For example, the _Escherichia coli_ Nissle 1917 strain was engineered to treat _P. aeruginosa_ infections in the gut[39], yet it cannot be used to treat respiratory infections because the respiratory tract is not its natural niche. _M. pneumoniae_ is the causative agent of atypical pneumonia and other extrapulmonary pathologies in humans. Compared with other bacterial chassis, _M. pneumoniae_ has the following advantages for treatment of lung infections: (1) it has a small genome (816 kbp); (2) it is a mild pathogen that can be eliminated with available antibiotics; (3) it is a bacterium for which more quantitative and extensive datasets are available[40–45]; (4) it has reduced metabolic and genetic networks[46], which reduce the risk of unwanted interference of the engineered circuits; (5) as it lacks a cell wall, it does not trigger a strong inflammatory response and can be combined with antibiotics that attack the peptidoglycan layer present in cell walls of pathogens (as shown in the present study); (6) its main antigens and virulence factors are well characterized[44,47–49]; (7) genetic tools are available to engineer its genome and to obtain an attenuated strain[50–52]; (8) some _M. pneumoniae_ strains, including M129, have a negligible rate of recombination, thereby reducing the risk of horizontal transfer; (9) its UGA codon encodes for tryptophan instead of a translation stop, providing an intrinsic biocontainment mechanism; and (10) it can be grown in a defined,

synthetic, serum-free medium to upscale its good manufacturing practice-compliant production[53].

We used an engineered, attenuated version of _M. pneumoniae_ M129 strain as a bacterial chassis to treat/prevent infectious lung diseases caused by _P. aeruginosa_. We first characterized in vivo the safety of use and survival of different attenuated _M. pneumoniae_ M129 strains in mouse lungs, to define the optimal chassis. We then engineered this nonpathogenic chassis by introducing two optimized genetic systems: one that combines biofilm dispersal activities (the glycoside hydrolases PelAh[54] and PslGh[55] and the A1-II′ alginate lyase[56]) and another that implements antimicrobial activity (pyocin L1 (ref. [57]) or pyocin S5 (ref. [58])) against biofilms formed by _P. aeruginosa_. We validated the activity of the engineered chassis strain in vitro, ex vivo and in vivo. We showed that the engineered strain can reduce an acute _P. aeruginosa_ infection in the murine model, thereby improving mouse survival, dissolve biofilms formed in vivo on ETTs in patients with VAP and be combined with antibiotics targeting the bacterial cell wall. Thus, it represents a promising alternative modality for preventing or treating biofilm-associated diseases and eradicating bacterial antibiotic resistance.

Results

Delivery and clearance of _M. pneumoniae_ strains in murine lung

We first studied the survival of the _M. pneumoniae_ wild-type (WT) strain in lungs. CD1 mice were inoculated intratracheally (i.t.) or intranasally and the bacterial load was determined in lung and bronchoalveolar lavage fluid (BALF) at 2 d postinfection (d.p.i.) (Extended Data Fig. 1a). As the highest bacterial load was detected in lung samples via the intratracheal route, we used intratracheal administration for the remaining experiments. In lungs, the bacterial load decreases at 4 d.p.i. and 14 d.p.i. compared with 2 dpi (2 and 4($\log_{10}$), respectively) (Extended Data Fig. 1b,c), indicating that _M. pneumoniae_ is cleared at 14 d.p.i.

Next, we sought to engineer an improved _M. pneumoniae_ strain by removing pathogenic genes. The following genes have been suggested as being responsible for _M. pneumoniae_ pathogenesis: _mpn372_ which encodes the community-acquired respiratory distress syndrome toxin[48,59]; _mpn133_ which encodes a lipoprotein with cytotoxic nuclease activity[49]; _mpn453_ which encodes the P30 adhesin protein[60]; and _mpn051_ which encodes the glycerol-3-phosphate dehydrogenase/oxidase (GlpD or GlpO)[47]. We previously showed that the Δ_mpn051_ strain grows poorly in vitro[46], because the GlpD enzyme is needed for _M. pneumoniae_ to use phosphatidylcholine as a carbon source in the lungs[61]. Also, recently we showed that an _M. pneumoniae_ strain harboring deletions in the _mpn372_ and _mpn133_ genes (CV2 strain) was attenuated in a mammary gland infection model[62]. As attenuation can differ in the respiratory tract, and other factors such as adhesion could affect virulence, we characterized the deletion of _mpn453_ as an additional gene to be removed to obtain an attenuated lung chassis. In the present study, we observed that the nonadherent Δ_mpn453_ strain has a significant reduction of colony-forming units (c.f.u.) recovered at 2 or 4 d.p.i. in mouse lungs compared with the WT strain (Extended Data Fig. 1b), suggesting that attachment to the epithelium is critical for maintenance of _M. pneumoniae_ in the lung. Thus, as a compromise between attenuation and maintenance in lungs, we selected, as an
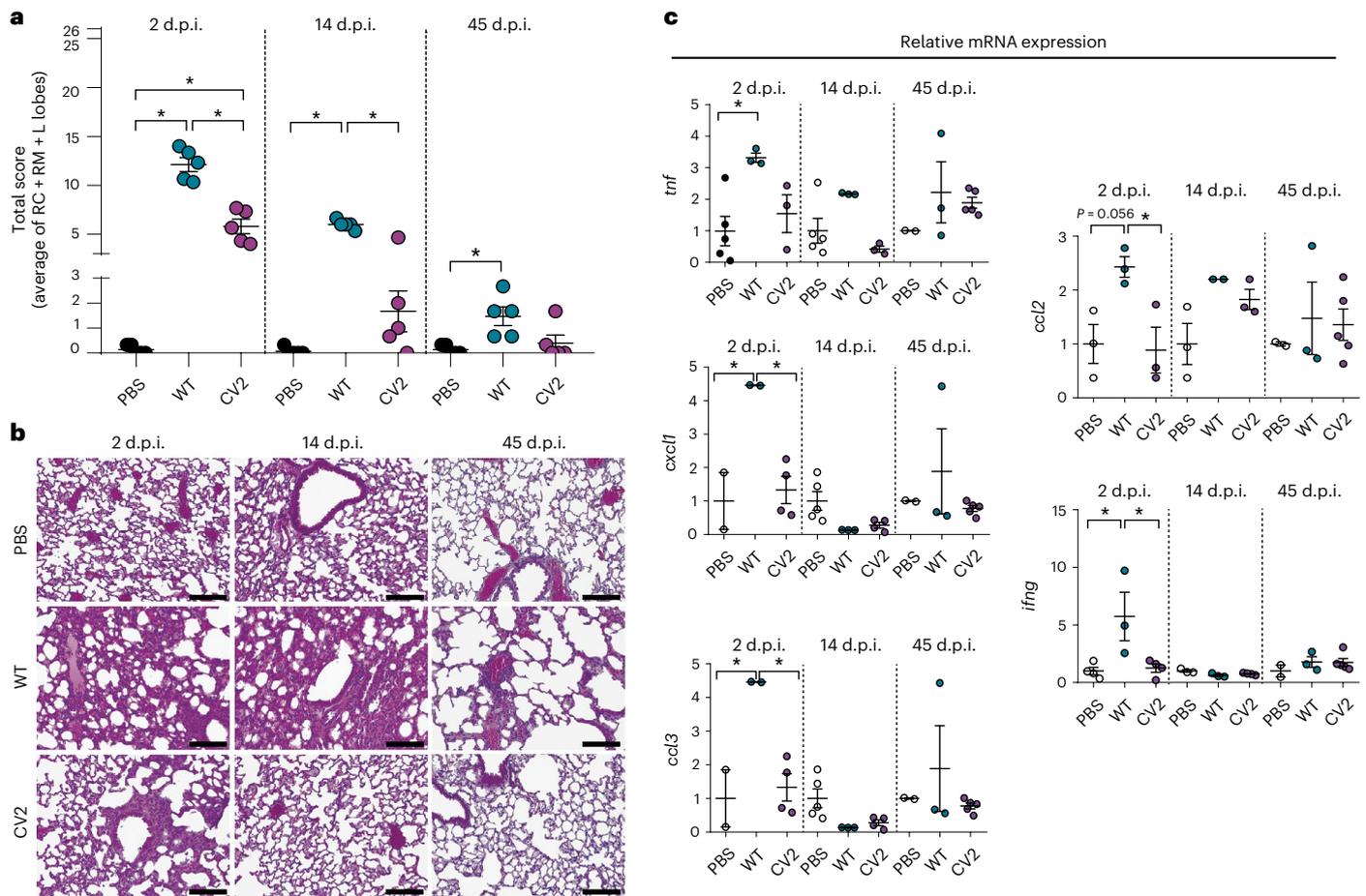
Fig. 1 | Tissue lesions and inflammatory response of lungs infected with *M. pneumoniae* WT and CV2 strain. CD1 mice (*n* = 5) were inoculated i.t. with *M. pneumoniae* CV2, WT or PBS (as control), and lungs were analyzed at 2, 14 and 45 d.p.i. **a**, Lung lesion evaluation, expressed as the total final score of the histological analysis performed on three major lobes. Each datapoint represents the average of the total score of the right cranial (RC), right middle (RM) and left lobes (L lobes). The mean values of each experimental group ± s.d. are indicated. *P < 0.05 by one-way ANOVA + Tukey's multiple-comparison test. For a detailed description of the scoring system used in the histopathological analysis, see Methods. **b**, Representative H&E-stained lung sections (200×) from the left lobe. Scale bar, 100 μm. **c**, Gene expression of inflammatory markers, assessed by RT–qPCR. Data are shown as mean ± s.d. of $2^{-\Delta\Delta Ct}$. *P < 0.05 by one-way ANOVA + Tukey's multiple-comparison test.

attenuated chassis for lung therapy, the CV2 strain, which harbors deleted *mpn372* and *mpn133* genes and WT *mpn453* and *mpn051* genes.

We tested the potential of lung colonization of the CV2 chassis compared with the WT strain by infecting animals i.t. with 1×10^7 c.f.u. (Extended Data Fig. 1c and Table 1). We obtained similar bacterial counts for WT and CV2 strains at 2, 4 and 14 d.p.i., indicating that deletion of *mpn372* and *mpn133* genes did not affect the CV2 capability of colonizing the lung.

Lung lesions and inflammatory response induced by the CV2 strain

To compare the response induced by CV2 and WT strains, we inoculated mice with a dose of 1×10^7 c.f.u. and then analyzed lungs at 2, 14 and 45 d.p.i. We determined the bacterial load in the lung tissue by quantifying the colony-forming units. In addition, lesions and immune response were evaluated by histopathology and cytokine profile, respectively. Of note, we found no statistical differences in the recovered colony-forming units between strains at different days postinfection and in different lung lobes (Extended Data Fig. 2a). This result showed a homogeneous distribution of the *M. pneumoniae* strain when inoculated i.t. and corroborated that deletion of genes in the CV2 strain did not affect its lung survival rate.

We then evaluated pulmonary lesions by histopathological analyses of three major lung lobes (right cranial, right middle and left lobe) using five parameters: (1) presence of peribronchial/peribronchiolar inflammatory infiltrate (%); (2) intensity of peribronchial/peribronchiolar inflammatory infiltrate; (3) intensity of bronchial/bronchiolar luminal exudate; (4) presence of perivascular inflammatory infiltrate (%); and (5) interstitial pneumonia intensity[63]. Based on these parameters, and as previously described[62,63], a final total score of up to 26 points was calculated as a global indicator of the lung lesion (Fig. 1a,b, Extended Data Fig. 2b and Supplementary Table 1). More details on the scoring system are given in Methods.

At 2 d.p.i., the total score indicated significantly milder lesions in the CV2 mice compared with the WT infected group (5.8 and 12.1 average points, respectively), with less peribronchiolar and perivascular inflammation and markedly less interstitial inflammation. At 14 d.p.i., the CV2 group showed no significant differences compared with the phosphate-buffered saline (PBS) control group, whereas the WT had remnant tissue injuries related to peribronchiolar, perivascular and interstitial inflammation (score of 6 in the WT versus 1.7 in CV2). At 45 d.p.i., the analyses indicated resolution of lung lesions in both CV2 and WT administered groups (except for perivascular infiltrate, which, although statistically not significant, was still high).
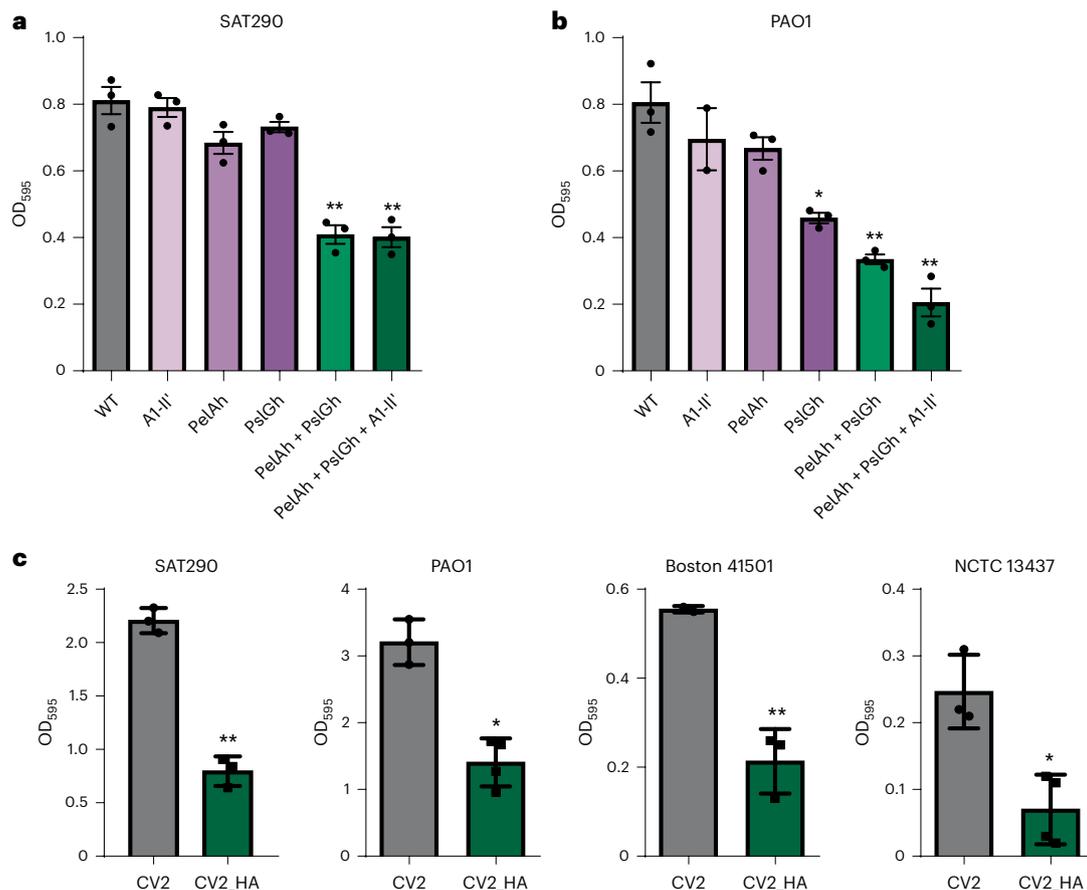
Fig. 2 | Biofilm dispersion activity of *M. pneumoniae* strains. The activity of the supernatants from *M. pneumoniae* strains against biofilms of the indicated *P. aeruginosa* strains (SAT290, PAO1, Boston 41501, NCTC3437) was assessed by Crystal Volet assay. Briefly, *Pseudomonas* biofilms were generated by seeding in 96-well plates and incubating at 37 °C for 24 h. Biofilms were then treated at 37 °C for 4 h with *M. pneumoniae* supernatants to allow the activity of the dispersal enzymes. More details are given in Methods. **a**,**b**, Biofilm dispersal activity of the supernatants of *M. pneumoniae* strains expressing the indicated heterologous proteins, tested against biofilms of SAT290 (a) or PAO1 (b) strains. **c**, Biofilm dispersal activity of the supernatants of CV2 and CV2_HA. Data are shown as the mean of three independent experiments ± s.d. $^*P < 0.05$, $^{**}P < 0.01$ by two-sided Student's *t*-test compared with the control strain. For details (for example, inoculum, growth and time), see Methods.

We next studied the induced inflammatory response by evaluating the expression of inflammatory markers in lungs by reverse transcription quantitative PCR (RT–qPCR; Fig. 1c, Extended Data Fig. 2c and Supplementary Table 2). The following panel of genes was analyzed: *il1b*, *il6*, *il12a*, *il23a*, *ifng*, *tnf*, *ccl2*, *ccl3* and *cxcl1*. We did not observe a significant induction of the *il1b*, *il6*, *il12a* and *il23a* genes by WT and CV2 (Extended Data Fig. 2c). In general, the response of the remaining markers was not high, although differences between CV2 and WT were observed. At 2 d.p.i., the WT strain induced expression of the inflammatory markers *tnf*, *cxcl1*, *ccl3*, *ccl2* and *ifng* compared with the PBS control mice, whereas CV2 did not induce any marker compared with WT mice. At 14 and 45 d.p.i., and in agreement with the histopathological analysis, the inflammatory response in both WT and CV2 lungs decreased to levels observed in PBS control mice (Fig. 1c).

Taken together, these results demonstrated that CV2 was attenuated in the lungs compared with the WT *M. pneumoniae* strain, underscoring it as a strong candidate for further engineering as a chassis to treat respiratory diseases.

Engineering an *M. pneumoniae* strain to dissolve *P. aeruginosa* biofilms

To introduce properties into our chassis to treat pulmonary infectious diseases, we designed and characterized an optimal genetic system for dispersing *P. aeruginosa* biofilms, which is one of the main pathogenic bacteria causing VAP. As the *P. aeruginosa* biofilm is mainly composed of the polysaccharides Pel, PsI and alginate, we engineered the WT strain with a genetic cassette expressing three different enzymes that target these three polysaccharides, namely: the glycoside hydrolases PelAh[64] and PsIGh[55], and the A1-II' alginate lyase[56], fused to a peptide for secretion (MPN142_OPT)[62] (European patent 16706622.4; Supplementary Table 3). First, we confirmed the expression of PelAh, PsIGh and A1-II' in the cell lysate and supernatant of CV2_HA by mass spectroscopy (MS; Supplementary Table 4). We then tested the antibiofilm activity of the supernatants of the different *M. pneumoniae* strains expressing either single enzymes or some of the possible combinations of enzymes against *P. aeruginosa* by Crystal Violet assay. We found that the *M. pneumoniae* strain engineered with a combination of the three enzymes showed the best dispersal activity against biofilms formed by *P. aeruginosa* strains SAT290 and PAO1 (Fig. 2a,b). We obtained similar results when using Alcian Blue as an alternative biofilm-staining method (Extended Data Fig. 3a). Hence, we included PelAh, PsIGh and A1-II' in the attenuated CV2 strain, CV2_HA. Finally, we confirmed the antibiofilm activity of CV2_HA in a panel of clinical *P. aeruginosa* strains (Fig. 2c). These results demonstrated that the *M. pneumoniae* strain CV2, which expresses and secretes the glycoside hydrolases PelAh and PsIGh and the A1-II' alginate lyase, degrades *P. aeruginosa* biofilms in vitro.
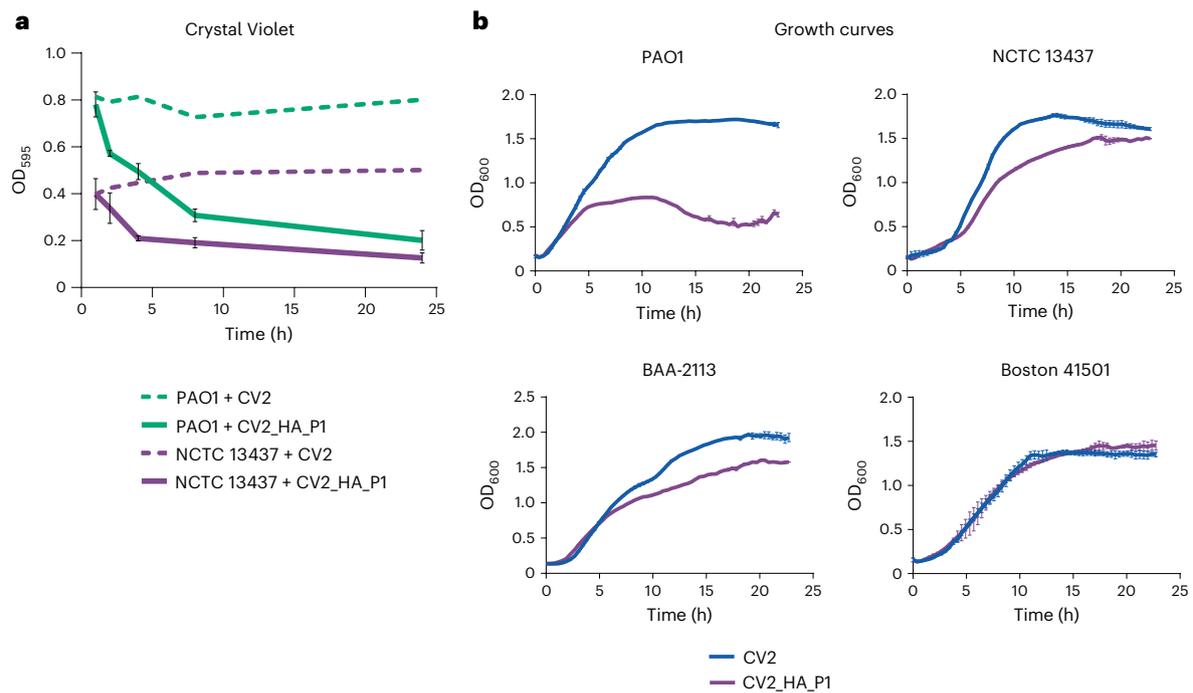
Fig. 3 | Biofilm dispersion and antimicrobial activities of the CV2_HA_P1 strain in vitro. a, Biofilm dispersal activity of the supernatant of strains CV2 (dashed lines) or CV2_HA_P1 (solid lines), assessed by Crystal Violet assay. *Pseudomonas* biofilms were generated in 96-well plates at 37 °C for 24 h and then treated at 37 °C with the indicated supernatants. Data are shown as the mean of three independent experiments ± s.d. with three technical replicates at each timepoint. **b**, Growth curves of different *P. aeruginosa* strains treated with supernatants from CV2 or CV2_HA_P1. Absorbance of the culture (OD_{600}) was measured every 20 min with a TECAN reader over 24 h. Errors bars indicate the s.d. of four replicates. For details (for example, inoculum, growth and time), see Methods.

Table 2 | Susceptibility of *M. pneumoniae* and *P. aeruginosa* strains SAT290, PAO1 and C117 to different antibiotics

Antibiotic	Target	*M. pneumoniae* CV2_HA		*P. aeruginosa* SAT290		PAO1		*P. aeruginosa* C117	
		Nonlethal	Lethal	Nonlethal	Lethal	Nonlethal	Lethal	Nonlethal	Lethal
Piperacillin/tazobactam	Cell wall	500	Nonlethal	ND	5	50	100	200	500
Ciprofloxacin	DNA gyrase	ND	50	ND	50	ND	50	50	100
Levofloxacin	DNA gyrase	ND	20	ND	20	20	200	20	200
Meropenem	Cell wall	500	Nonlethal	ND	1	1	10	10	100
Imipenem/cilastatin	Cell wall	500	Nonlethal	ND	5	5	30	5	300
Amikacin	Ribosome	ND	10	10	100	ND	10	10	100
Ceftacidime/avibactam	Cell wall	15	Nonlethal	0.5	15	5	15	15	ND
Ceftolozane/tazobactam	Cell wall	15	Nonlethal	ND	0.5	0.5	5	15	ND

Inoculum, growth and time are detailed in Methods. Numbers in the table represent the concentrations tested ($\mu g\,ml^{-1}$) of each antibiotic. ND, Not determined.

Addition of antimicrobial activity to CV2_HA

The ideal engineered *M. pneumoniae* strain to treat VAP should combine biofilm dispersal and antimicrobial activity. To introduce antimicrobial activity, we engineered CV2_HA to express the bacteriocin pyocin L1 (CV2_HA_P1), which was previously shown to kill some *P. aeruginosa* strains, including PAO1 (ref. [57]). First, we confirmed the capacity of the cell-free supernatant of CV2_HA_P1 to dissolve biofilms formed by two different *P. aeruginosa* strains by Crystal Violet (Fig. 3a) and also the colony-forming unit count (Extended Data Fig. 3b). Then, we characterized the antimicrobial properties of CV2_HA_P1 on four different *P. aeruginosa* strains. We found that CV2_HA_P1 inhibited the growth of PAO1 and showed moderate activity against NCTC13437 and BAA-2113 strains but not against the Boston 41501 strain (Fig. 3b and Extended Data Fig. 3c). To diversify the antimicrobial spectrum, we expressed

pyocin S5 (ref. [55]) instead of pyocin L1, which led to growth inhibition of the *P. aeruginosa* Boston strain (Extended Data Fig. 4a).

These results demonstrated that (1) the strain CV2_HA_P1 displayed both antibiofilm and antimicrobial activities against *P. aeruginosa* and (2) the antimicrobial activity of the engineered *M. pneumoniae* can be modulated to act against specific *P. aeruginosa* strains by introducing different antimicrobial pyocins.

Effects of CV2_HA_P1 in ETTs from VAP patients

As *M. pneumoniae* lacks a cell wall, we speculated that it could be used in combination with antibiotics targeting the peptidoglycans of the cell wall of both Gram-positive and Gram-negative bacteria. To test this hypothesis, we evaluated the effect on the growth of *M. pneumoniae* and different *P. aeruginosa* strains of antibiotics commonly used in
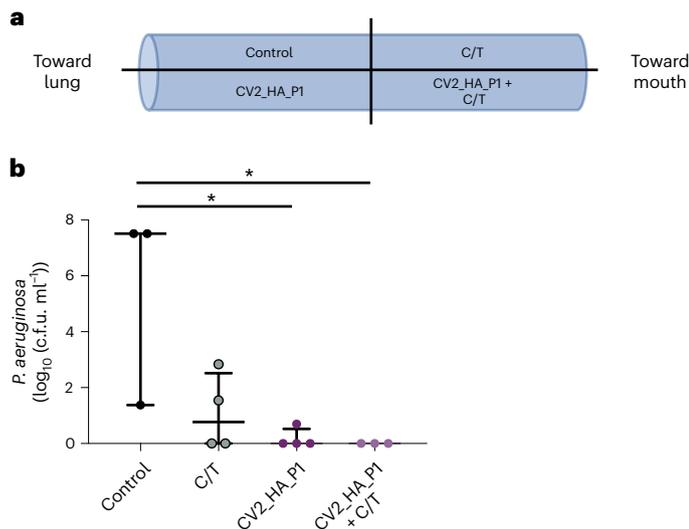
a

b

Fig. 4 | Dispersion of biofilms of ETTs from patients with VAP. a, Schematic representation of ETT slices from patients in the ICU who received MV. The 4-cm ETTs were taken from the distal part (for example, the first 10 cm closest to the patient's lungs) and were sliced into four hemisections. One hemisection was used for each treatment arm: control (Hayflick medium alone without treatment), CV2_HA_P1 (-1 × 10^8 cells), C/T (5 μg ml^{-1}) or CV2_HA_P1 + C/T. **b**, Effect on the *P. aeruginosa* load on ETT biofilm from patients who received MV (see Methods). Significant differences between groups were found: *P* = 0.049 by two-sided Kruskal–Wallis test. The median and the IQR load (log$_{10}$(c.f.u. ml^{-1})) of each treatment group were: (1) control (*n* = 3): 7.51 (4.44–7.51); (2) C/T (*n* = 4): 0.77 (0.00–2.52); (3) CV2_HA_P1 (*n* = 4): 0.00 (0.00–0.52); and (4) CV2_HA_P1 + C/T (*n* = 3): 0.00 (0.00–0.00). The *P* values for pairwise comparisons between groups (Wilcoxon's signed-rank test) are indicated when significant (*P* < 0.05). The level of significance for pairwise comparisons was *P* = 0.008.

clinics (Table 2 and Extended Data Fig. 4b). As expected, we found that no antibiotics that target the cell wall killed the CV2_HA strain, whereas all the antibiotics were active against most *P. aeruginosa* strains (Table 2). Of note, although the antibiotics did not dissolve *P. aeruginosa* biofilms to any significant degree, incubation with the CV2_HA_P1 strain effectively dissolved the biofilm (Extended Data Fig. 4c).

To evaluate the efficacy of our CV2_HA_P1 strain in dissolving in vivo-formed biofilms, we treated sections of ETTs obtained from VAP patients receiving mechanical ventilation in the ICU (see Methods). After a median of 11 d of MV, *P. aeruginosa* biofilms were observed on the ETTs, with bacterial loads of approximately 2.57 (2.20–4.81) log$_{10}$(c.f.u. ml^{-1}). The *P. aeruginosa* strains in the ETTs showed resistance to meropenem (100%), imipenem (100%), aztreonam (100%), amikacin (66%) and ciprofloxacin (33%), but were susceptible to colistin, piperacillin/tazobactam, tobramycin and ceftazidime. Multilocus sequence-type analysis of *P. aeruginosa* identified the ST109 and ST259 strains, which are allocated to the clonal complexes 253 and 2044. Complex 253 was previously identified from patients on the ICU[65] and the complex 2044 was found in patients with bronchiectasis.

We included 14 of the 16 ETT sections in the final analysis, distributed as follows in each treatment group: control (*n* = 3), ceftolozane/tazobactam (C/T) (*n* = 4), CV2_HA_P1 (*n* = 4) and CV2_HA_P1 + C/T (*n* = 3; Fig. 4a); the remaining two samples were discarded because no *P. aeruginosa* counts could be obtained due to overgrowth of *Proteus* spp. After a 24-h incubation, the *P. aeruginosa* load showed significant differences between the control and the treated groups (Fig. 4b): ETT biofilms treated with antibiotics reduced the *P. aeruginosa* load and this reduction was even more substantial with the CV2_HA_P1 alone or in combination with the C/T antibiotics. These results demonstrate

that CV2_HA_P1 has broad-spectrum activity against biofilms formed by different multidrug-resistant *P. aeruginosa* clinical strains.

Efficacy of CV2_HA_P1 in a murine lung infection model

To study the efficacy of CV2_HA_P1 in vivo, we first tested its toxicity by inoculating mice with 1 × 10^8 c.f.u. and analyzing lungs at 2, 14 and 45 d.p.i. by histopathology and cytokine measurement (Extended Data Fig. 5 and Supplementary Tables 5 and 6).

At 2 d.p.i., the same bacterial load was recovered in lungs of WT and CV2_HA_P1 strains; however, the CV2_HA_P1 lungs showed significantly fewer alterations compared with the WT group (*P* < 0.05). At 14 and 45 d.p.i., no colony-forming units were detected in CV2_HA_P1 lungs and the total score of the histopathology was not significantly different from the PBS controls; in stark contrast, WT infected lungs still presented tissue lesions (Extended Data Fig. 5a–c and Supplementary Table 5). Study of inflammation markers corroborated the resolution of lesions and the attenuation of the engineered CV2_HA_P1 strain (Extended Data Fig. 5d and Supplementary Table 6).

Next, we established a murine model of acute lung infection using PAO1. We immunosuppressed mice with cyclophosphamide and inoculated i.t. different amounts of the *P. aeruginosa* PAO1 strain (*n* = 8 mice for each group). Mouse survival, body weight and clinical conditions were assessed at different time points (Extended Data Fig. 6a–d). Mice infected with doses >1 × 10^4 c.f.u. had to be sacrificed or died at 12 h post-inoculation (h.p.i.); mice infected with 5 × 10^3 and 1 × 10^4 c.f.u. survive until 18 h.p.i. (Extended Data Fig. 6b), at which point the clinical score was 4 (Extended Data Fig. 6c; see Methods), and mice infected with 1 × 10^3 c.f.u. survived until 24 h.p.i. with a final clinical score of 2 and died by 48 h.p.i. Based on these results, we decided to use an inoculum of 1 × 10^3 c.f.u. per mouse of PAO1, which ensured lung colonization of the infected mice without treatment and survival for a longer period, thereby allowing the therapeutic effect of our chassis to be monitored.

Next, we studied the efficacy of CV2_HA_P1 in reducing the PAO1 load in the established lung infection model (Fig. 5a). We infected mice with the PAO1 strain, 1 × 10^3 c.f.u. per mouse (as described above), and treated them at 2 h.p.i. with different amounts (1 × 10^7 or 1 × 10^8 c.f.u.) of CV2_HA_P1, CV2 or PBS. All mice in the groups survived to 26 h.p.i., at which point they showed decreased body weight and clinical score 2, but no other signs of clinical deterioration. After sacrifice at 26 h.p.i., we counted the bacterial burden in the lungs. CV2 and CV2_HA_P1 colony-forming units were detected in the lungs (Extended Data Fig. 7), indicating that *M. pneumoniae* can colonize the lungs in the presence of a more severe pathogenic bacterium such as *P. aeruginosa*. The mean burden of PAO1 in the PBS control was 1 × 10^6 c.f.u. per g of lung tissue. Mice treated with CV2_HA_P1 at 1 × 10^8 c.f.u. had a significant reduction in the PAO1 load in the lungs compared with the PBS or CV2 control (reduction of 3.65log$_{10}$ and 4.39log$_{10}$, respectively; Fig. 5b). CV2 did not significantly reduce the PAO1 burden in the lungs compared with vehicle or pretreatment control groups at any time. We also studied the histopathology of the lungs at this timepoint. In agreement with the reduction of the PAO1 load, we observed that the total score of lung lesions was significantly lower in the lungs of mice treated with CV2_HA_P1 compared with the controls (Fig. 5c), with less perivascular inflammation and markedly less parenchymal pneumonia. Inflammation markers were also reduced in the lungs of CV2_HA_P1 mice compared with the CV2 group (Fig. 5d). These data indicated that CV2_HA_P1 treatment reduced the PAO1 lung infection in an in vivo model of acute pneumonia.

To study the effect of the CV2_HA_P1 therapy beyond 26 h.p.i., we next analyzed the survival of the mice over days after infection with PAO1 (Fig. 5e). About 50% of mice infected with PAO1 and treated with CV2_HA_P1 survived up to 8 d.p.i. (with a median of 7 d.p.i.), whereas mice treated with the CV2 or PBS control had a median survival of 2 d.p.i. Moreover, histology of mice with PAO1 infection that survived to the 8-d.p.i. timepoint revealed substantially fewer lung alterations
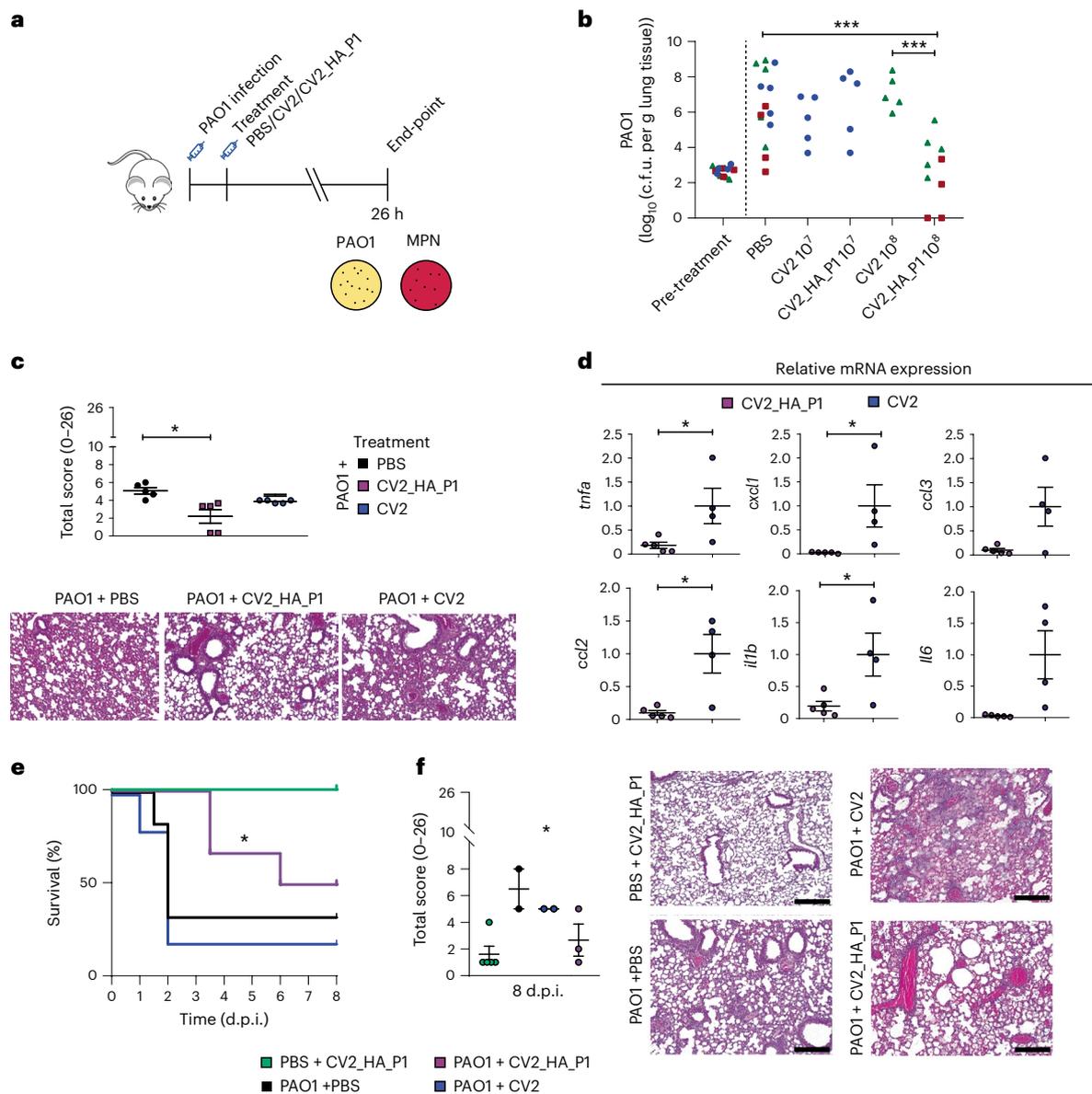
Fig. 5 | In vivo treatment of mice with acute respiratory PAO1 infection. a, CD1 mice immunocompromised with cyclophosphamide and infected i.t. with 1×10^3 c.f.u. of *P. aeruginosa* PAO1. At 2 h.p.i., mice were treated i.t. with 1×10^7 (experiment (exp.) 1) or 1×10^8 (exp. 2 and 3) c.f.u. of CV2_HA_P1 *M. pneumoniae* strains or CV2 strain, or PBS. MPN: *M. pneumoniae*. At 26 h.p.i., mice were sacrificed to determine the PAO1 load in the lungs after the treatments (more details in Methods). **b,** Colony-forming units for *P. aeruginosa* PAO1 found in different treatment conditions. Three independent experiments were performed, indicated by different symbols in the graph: exp. 1 (blue circles), exp. 2 (red squares) and exp. 3 (green triangles). In each experiment, five mice were used per treatment group. Five additional mice were kept untreated and sacrificed to determine the PAO1 load in the lungs before the treatments (pretreatment control). $^{***}P < 0.001$ by two-sided Student's *t*-test. **c,** Lung lesion evaluation (total score) of mice infected with PAO1 and treated with the indicated *M. pneumoniae* strains. $^*P < 0.05$ by one-way ANOVA + Tukey's multiple-comparison test. Histological analysis was performed on three major lobes (right

cranial, right middle and left). See Methods for further detailed description of the scoring system used in the histopathological analysis. Below, representative H&E-stained lung sections (100×) from the left lobe. Scale bar, 100 μm. **d,** Relative gene expression of inflammatory markers, assessed by RT–qPCR of lung homogenates. Each animal used is marked as an individual dot (CV2, $n = 4$; CV2_HA_P1, $n = 5$). Data are shown as mean ± s.d. of $2^{-\Delta\Delta Ct}$. $^*P < 0.05$ by two-sided Student's *t*-test. **e,** Survival of mice infected with PAO1 and treated with CV2_HA_P1 or controls. $^*P = 0.0357$ by Gehan–Breslow–Wilcoxon test with comparison to CV2 control. **f,** Lung lesions assessed by histological analysis of the lungs of the animals that survived until 8 d.p.i. ($n = 5$ for PBS + CV2_HA_P1 control; $n = 2$ for PAO1 + PBS and for PAO1 + CV2 groups; $n = 3$ for PAO1 + CV2_HA_P1 group). See Methods for details of the scoring. $^*P = 0.0189$ by one-way ANOVA + Bonferroni's test. Right, representative H&E-stained lung sections (100×) from the left lobe, obtained using a digital camera (MC170 HD, Leica) connected to an optical microscope (DM2000, Leica) using a commercial software (Leica Application Suite, v.4.6.0). Scale bar, 100 μm.

in the CV2_HA_P1 group than in the CV2 or PBS control groups (Fig. 5f). These data indicated that CV2_HA_P1 treatment reduced PAO1 lung infection and increased mouse survival.

We also studied the efficacy of CV2_HA_P1 as a prophylactic treatment against PAO1 infection (Extended Data Fig. 8a). We inoculated

mice with a mix of *M. pneumoniae* (WT_HA_P1 or CV2_HA_P1; doses 1×10^5 or 1×10^7 c.f.u., respectively) and PAO1, and we studied the progression of PAO1 infection up to 8 d.p.i. *M. pneumoniae* colony-forming units in the lungs were recovered from all groups (Extended Data Fig. 8b). PAO1 colony-forming units were significantly reduced in the lungs of

mice treated with 1×10^7 c.f.u. of WT_HA_P1 or CV2_HA_P1 strains compared with nontreated control mice (Extended Data Fig. 8c).

Taken together, these results demonstrated that our engineered *M. pneumoniae* strain CV2_HA_P1 was efficient in treating acute PAO1 infections in a mouse model.

Discussion

Lung infections, one of the major causes of human mortality, represent an untapped target for bacterial therapeutics. In the present study, we have shown that an engineered strain of the genome-reduced human lung bacterium *M. pneumoniae* (CV2) is attenuated in the lung and can be used to treat respiratory diseases associated with biofilm formation, such as VAP. The CV2 strain produces mild lesions in the acute phase of the lung infection that are resolved, avoiding chronic damage to the lung tissue, having an attenuated inflammation response and being removed spontaneously from the mouse lung after 4 d.p.i.

To demonstrate the potential use of our chassis to treat infectious lung diseases, we introduced genes to dissolve biofilms made by *P. aeruginosa* and to kill this bacterium. The biofilm matrix of *P. aeruginosa* PAO1 comprises DNA, proteins and the polysaccharides Pel and Psl[54–56]; alginate is also a main component of the biofilm of mucoid *P. aeruginosa* strains[12,56]. PelAh and PslGh have been reported as optimal enzymes for degradation of Pel and Psl exopolysaccharides, respectively[55,64]. The alginate lyase enzyme AI-II′, with both poly(M) and poly(G) activities, is effective against biofilms of *P. aeruginosa* mucoid strains[56]. We found that the strain expressing the three enzymes (CV2_HA) was effective in dissolving biofilms formed by different mucoid strains of *P. aeruginosa*. As it was previously reported that combining dispersal and antimicrobial activities could enhance biofilm degradation[56,62], we engineered *M. pneumoniae* to express active pyocin L1 and pyocin S5. Both pyocins were active and specific for the target strains. We decided to use the *M. pneumoniae* strain expressing pyocin L1 (CV2_HA_P1), which proved to have an effective antimicrobial activity against *P. aeruginosa* PAO1 infection (which we used in the in vivo mouse infection model). We demonstrated the efficacy of our CV2_HA_P1 strain in dissolving biofilms on ETTs from patients in ICU who had received MV for long periods. We also observed that we could rescue the efficacy of standard-of-care antibiotics that were not efficient because of biofilm when combined with CV2_HA_P1, which opens the way for synergistic combinations.

In a mouse model of acute *P. aeruginosa* PAO1 infection, CV2_HA_P1 treatment eliminated the infection at 26 h.p.i. and increased the survival rate of the treated mice. No adverse clinical symptoms were observed related to body weight loss, fever, piloerection or respiratory distress, suggesting that treatment with CV2_HA_P1 at a high single dose was effective without toxicity for up to 8 d.p.i. In addition, CV2_HA_P1 showed a prophylactic effect against *P. aeruginosa* biofilm in vivo, expanding its potential clinical applications.

In conclusion, we have provided evidence that a lung biotherapeutic bacterial strain is effective against biofilm-associated infections in the respiratory tract. We envision that our CV2 chassis could be adapted for the treatment of other infectious and noninfectious lung diseases that require continuous local delivery of therapeutic molecules.

Online content

Any methods, additional references, Nature Portfolio reporting summaries, source data, extended data, supplementary information, acknowledgements, peer review information; details of author contributions and competing interests; and statements of data and code availability are available at https://doi.org/10.1038/s41587-022-01584-9.

References

1. Wang, S., Gao, Y., Jin, Q. & Ji, J. Emerging antibacterial nanomedicine for enhanced antibiotic therapy. *Biomater. Sci.* **8**, 6825–6839 (2020).
2. Helaly, A. M. N., El-Attar, Y. A., Khalil, M., Ahmed Ghorab, D. S. E.-D. & El-Mansoury, A. M. Antibiotic abuse induced histopathological and neurobehavioral disorders in mice. *Curr. Drug Saf.* **14**, 199–208 (2019).
3. Høiby, N., Bjarnsholt, T., Givskov, M., Molin, S. & Ciofu, O. Antibiotic resistance of bacterial biofilms. *Int. J. Antimicrob. Agents* **35**, 322–332 (2010).
4. Obst, U., Schwartz, T. & Volkmann, H. Antibiotic resistant pathogenic bacteria and their resistance genes in bacterial biofilms. *Int. J. Artif. Organs* **29**, 387–394 (2006).
5. Smith, A. W. Biofilms and antibiotic therapy: is there a role for combating bacterial resistance by the use of novel drug delivery systems? *Adv. Drug Deliv. Rev.* **57**, 1539–1550 (2005).
6. Stewart, P. S. Mechanisms of antibiotic resistance in bacterial biofilms. *Int. J. Med. Microbiol.* **292**, 107–113 (2002).
7. del Pozo, J. L. & Patel, R. The challenge of treating biofilm-associated bacterial infections. *Clin. Pharmacol. Ther.* **82**, 204–209 (2007).
8. Welp, A. L. & Bomberger, J. M. Bacterial community interactions during chronic respiratory disease. *Front. Cell Infect. Microbiol.* **10**, 213 (2020).
9. Orazi, G. & O'Toole, G. A. *Pseudomonas aeruginosa* alters *Staphylococcus aureus* sensitivity to vancomycin in a biofilm model of cystic fibrosis infection. *mBio* **8**, e00873-17 (2017).
10. Torres, A. et al. International ERS/ESICM/ESCMID/ALAT guidelines for the management of hospital-acquired pneumonia and ventilator-associated pneumonia: guidelines for the management of hospital-acquired pneumonia (HAP)/ventilator-associated pneumonia (VAP) of the European Respiratory Society (ERS), European Society of Intensive Care Medicine (ESICM), European Society of Clinical Microbiology and Infectious Diseases (ESCMID) and Asociación Latinoamericana del Tórax (ALAT). *Eur. Respir. J.* **50**, 1700582 (2017).
11. Ferrer, M. & Torres, A. Epidemiology of ICU-acquired pneumonia. *Curr. Opin. Crit. Care* **24**, 325–331 (2018).
12. Mann, E. E. & Wozniak, D. J. *Pseudomonas* biofilm matrix composition and niche biology. *FEMS Microbiol. Rev.* **36**, 893–916 (2012).
13. Luo, Y., Yang, Q., Zhang, D. & Yan, W. Mechanisms and control strategies of antibiotic resistance in pathological biofilms. *J. Microbiol. Biotechnol.* https://doi.org/10.4014/jmb.2010.10021 (2020).
14. Alhede, M. et al. Bacterial aggregate size determines phagocytosis efficiency of polymorphonuclear leukocytes. *Med. Microbiol. Immunol.* **209**, 669–680 (2020).
15. Bortone, B. et al. High global consumption of potentially inappropriate fixed dose combination antibiotics: analysis of data from 75 countries. *PLoS ONE* **16**, e0241899 (2021).
16. Fernández-Barat, L., López-Aladid, R. & Torres, A. Reconsidering ventilator-associated pneumonia from a new dimension of the lung microbiome. *eBioMedicine* **60**, 102995 (2020).
17. On behalf of the coVAPid Study Group et al. Relationship between SARS-CoV-2 infection and the incidence of ventilator-associated lower respiratory tract infections: a European multicenter cohort study. *Intens. Care Med.* https://doi.org/10.1007/s00134-020-06323-9 (2021).
18. Pickens, C. O. et al. Bacterial superinfection pneumonia in patients mechanically ventilated for COVID-19 pneumonia. *Am. J. Respir. Crit. Care Med.* **204**, 921–932 (2021).
19. Nseir, S. et al. Relationship between ventilator-associated pneumonia and mortality in COVID-19 patients: a planned ancillary analysis of the coVAPid cohort. *Crit. Care* **25**, 177 (2021).
20. Micek, S. T. et al. An international multicenter retrospective study of *Pseudomonas aeruginosa* nosocomial pneumonia: impact of multidrug resistance. *Crit. Care* **19**, 219 (2015).

21. Fernández-Barat, L. et al. Intensive care unit-acquired pneumonia due to *Pseudomonas aeruginosa* with and without multidrug resistance. *J. Infect.* **74**, 142–152 (2017).

22. Niederman, M. S. Adjunctive nebulized antibiotics: what is their place in ICU infections? *Front. Med.* **6**, 99 (2019).

23. Bermúdez-Humarán, L. G. et al. Engineering lactococci and lactobacilli for human health. *Curr. Opin. Microbiol.* **16**, 278–283 (2013).

24. Kuehn, M. J. Genetically engineered probiotic competition. *Gastroenterology* **130**, 1915–1916 (2006).

25. Durrer, K. E., Allen, M. S. & Hunt von Herbing, I. Genetically engineered probiotic for the treatment of phenylketonuria (PKU): assessment of a novel treatment in vitro and in the PAHenu2 mouse model of PKU. *PLoS ONE* **12**, e0176286 (2017).

26. Gupta, S., Bram, E. E. & Weiss, R. Genetically programmable pathogen sense and destroy. *ACS Synth. Biol.* **2**, 715–723 (2013).

27. Palma, M. L., Garcia-Bates, T. M., Martins, F. S. & Douradinha, B. Correction to: genetically engineered probiotic *Saccharomyces cerevisiae* strains mature human dendritic cells and stimulate gag-specific memory CD8+ T cells ex vivo. *Appl. Microbiol. Biotechnol.* **103**, 5461 (2019).

28. Steidler, L. et al. Biological containment of genetically modified *Lactococcus lactis* for intestinal delivery of human interleukin 10. *Nat. Biotechnol.* **21**, 785–789 (2003).

29. Martín, R. et al. Effects in the use of a genetically engineered strain of *Lactococcus lactis* delivering in situ IL-10 as a therapy to treat low-grade colon inflammation. *Hum. Vaccines Immunother.* **10**, 1611–1621 (2014).

30. Lalsiamthara, J., Kim, J. H. & Lee, J. H. Engineering of a rough auxotrophic mutant *Salmonella typhimurium* for effective delivery. *Oncotarget* **9**, 25441–25457 (2018).

31. Steidler, L. et al. Treatment of murine colitis by *Lactococcus lactis* secreting interleukin-10. *Science* **289**, 1352–1355 (2000).

32. Schotte, L., Steidler, L., Vandekerckhove, J. & Remaut, E. Secretion of biologically active murine interleukin-10 by *Lactococcus lactis*. *Enzyme Microb. Technol.* **27**, 761–765 (2000).

33. Vandenbroucke, K. et al. Orally administered *L. lactis* secreting an anti-TNF nanobody demonstrates efficacy in chronic colitis. *Mucosal Immunol.* **3**, 49–56 (2010).

34. Vandenbroucke, K. et al. Active delivery of trefoil factors by genetically modified *Lactococcus lactis* prevents and heals acute colitis in mice. *Gastroenterology* **127**, 502–513 (2004).

35. Liu, X. et al. Engineered vaginal lactobacillus strain for mucosal delivery of the human immunodeficiency virus inhibitor cyanovirin-N. *Antimicrob. Agents Chemother.* **50**, 3250–3259 (2006).

36. Liu, X., Lagenaur, L. A., Lee, P. P. & Xu, Q. Engineering of a human vaginal *Lactobacillus* strain for surface expression of two-domain CD4 molecules. *Appl. Environ. Microbiol.* **74**, 4626–4635 (2008).

37. Charbonneau, M. R., Isabella, V. M., Li, N. & Kurtz, C. B. Developing a new class of engineered live bacterial therapeutics to treat human diseases. *Nat. Commun.* **11**, 1738 (2020).

38. Kutter, E. et al. Phage therapy in clinical practice: treatment of human infections. *Curr. Pharm. Biotechnol.* **11**, 69–86 (2010).

39. De Smet, J., Hendrix, H., Blasdel, B. G., Danis-Wlodarczyk, K. & Lavigne, R. *Pseudomonas* predators: understanding and exploiting phage–host interactions. *Nat. Rev. Microbiol.* **15**, 517–530 (2017).

40. Trussart, M. et al. Defined chromosome structure in the genome-reduced bacterium *Mycoplasma pneumoniae*. *Nat. Commun.* **8**, 14665 (2017).

41. Wodke, J. A. H. et al. Dissecting the energy metabolism in *Mycoplasma pneumoniae* through genome-scale metabolic modeling. *Mol. Syst. Biol.* **9**, 653 (2013).

42. Lloréns-Rico, V. et al. Bacterial antisense RNAs are mainly the product of transcriptional noise. *Sci. Adv.* **2**, e1501363 (2016).

43. Lluch-Senar, M. et al. Defining a minimal cell: essentiality of small ORFs and ncRNAs in a genome-reduced bacterium. *Mol. Syst. Biol.* **11**, 780 (2015).

44. Lluch-Senar, M. et al. Comparative '-omics' in *Mycoplasma pneumoniae* clinical isolates reveals key virulence factors. *PLoS ONE* **10**, e0137354 (2015).

45. Burgos, R., Weber, M., Martinez, S., Lluch-Senar, M. & Serrano, L. Protein quality control and regulated proteolysis in the genome-reduced organism *Mycoplasma pneumoniae*. *Mol. Syst. Biol.* **16**, e9530 (2020).

46. Yus, E. et al. Determination of the gene regulatory network of a genome-reduced bacterium highlights alternative regulation independent of transcription factors. *Cell Syst.* **9**, 143–158.e13 (2019).

47. Blötz, C. & Stülke, J. Glycerol metabolism and its implication in virulence in *Mycoplasma*. *FEMS Microbiol. Rev.* **41**, 640–652 (2017).

48. Bose, S. et al. ADP-ribosylation of NLRP3 by *Mycoplasma pneumoniae* CARDS toxin regulates inflammasome activity. *mBio* **5**, e02186-14 (2014).

49. Somarajan, S. R., Kannan, T. R. & Baseman, J. B. *Mycoplasma pneumoniae* Mpn133 is a cytotoxic nuclease with a glutamic acid-, lysine- and serine-rich region essential for binding and internalization but not enzymatic activity. *Cell. Microbiol.* **12**, 1821–1831 (2010).

50. Garcia-Morales, L. et al. A RAGE based strategy for the genome engineering of the human respiratory pathogen *Mycoplasma pneumoniae*. *ACS Synth. Biol.* **9**, 2737–2748 (2020).

51. Piñero-Lambea, C. et al. *Mycoplasma pneumoniae* genome editing based on oligo recombineering and Cas9-mediated counterselection. *ACS Synth. Biol.* **9**, 1693–1704 (2020).

52. Piñero-Lambea, C. et al. SURE editing: combining oligo-recombineering and programmable insertion/deletion of selection markers to efficiently edit the *Mycoplasma pneumoniae* genome. *Nucleic Acids Res.* https://doi.org/10.1093/nar/gkac836 (2022).

53. Gaspari, E. et al. Model-driven design allows growth of *Mycoplasma pneumoniae* on serum-free media. *NPJ Syst. Biol. Appl.* **6**, 33 (2020).

54. Baker, P. et al. Exopolysaccharide biosynthetic glycoside hydrolases can be utilized to disrupt and prevent *Pseudomonas aeruginosa* biofilms. *Sci. Adv.* **2**, e1501632 (2016).

55. Pestrak, M. J. et al. Treatment with the *Pseudomonas aeruginosa* glycoside hydrolase PslG combats wound infection by improving antibiotic efficacy and host innate immune activity. *Antimicrob. Agents Chemother.* **63**, e00234-19 (2019).

56. Blanco-Cabra, N. et al. Characterization of different alginate lyases for dissolving *Pseudomonas aeruginosa* biofilms. *Sci. Rep.* **10**, 9390 (2020).

57. Ghequire, M. G. K. et al. O serotype-independent susceptibility of *Pseudomonas aeruginosa* to lectin-like pyocins. *MicrobiologyOpen* **3**, 875–884 (2014).

58. Elfarash, A. et al. Pore-forming pyocin S5 utilizes the FptA ferripyochelin receptor to kill *Pseudomonas aeruginosa*. *Microbiology* **160**, 261–269 (2014).

59. Becker, A. et al. Structure of CARDS toxin, a unique ADP-ribosylating and vacuolating cytotoxin from *Mycoplasma pneumoniae*. *Proc. Natl Acad. Sci. USA* **112**, 5165–5170 (2015).

60. Chang, H.-Y., Jordan, J. L. & Krause, D. C. Domain analysis of protein P30 in *Mycoplasma pneumoniae* cytadherence and gliding motility. *J. Bacteriol.* **193**, 1726–1733 (2011).

61. Schmidl, S. R. et al. A trigger enzyme in *Mycoplasma pneumoniae*: impact of the glycerophosphodiesterase GlpQ on virulence and gene expression. *PLoS Pathog.* **7**, e1002263 (2011).

62. Garrido, V. et al. Engineering a genome-reduced bacterium to eliminate *Staphylococcus aureus* biofilms in vivo. *Mol. Syst. Biol.* **17**, e10145 (2021).

63. Martin, R. J., Chu, H. W., Honour, J. M. & Harbeck, R. J. Airway inflammation and bronchial hyperresponsiveness after *Mycoplasma pneumoniae* infection in a murine model. *Am. J. Respir. Cell Mol. Biol.* **24**, 577–582 (2001).

64. Szymańska, M. et al. Glycoside hydrolase (PelAh) immobilization prevents *Pseudomonas aeruginosa* biofilm formation on cellulose-based wound dressing. *Carbohydr. Polym.* **246**, 116625 (2020).

65. Magalhães, B. et al. Combining standard molecular typing and whole genome sequencing to investigate *Pseudomonas aeruginosa* epidemiology in intensive care units. *Front. Public Health* **8**, 3 (2020).

Methods

Medium and strain growth conditions

Liquid Hayflick complete medium was prepared by mixing 800 ml of noncomplete medium A (20 g of PPLO broth (Difco, catalog no. 255420), 30 g of Hepes (100 mM final), 25 ml of 0.5% phenol red solution (Sigma-Aldrich, catalog no. P3532)), 200 ml of heat-inactivated horse serum (Life Technologies, catalog no. 26050088), 20 ml of sterile filtered 50% glucose and 1 ml of a 100-mg ml^{-1} stock of ampicillin (final concentration 100 μg ml^{-1}, ampicillin sodium salt; Sigma-Alrich, catalog no. A9518). Solid Hayflick 1% agar plates were prepared by mixing 800 ml of noncomplete medium A with 10 g of Bacto Agar (BD, catalog no. 214010) and adding 200 ml of heat-inactivated horse serum, 20 ml of sterile filtered 50% glucose and 1 ml of a 100-mg ml^{-1} stock of ampicillin (final concentration 100 μg ml^{-1}).

For *P. aeruginosa* growth curves, strains were grown overnight in Tryptic Soy Broth (TSB) medium at 37 °C with shaking. The next day, the cultures were diluted in TSB to absorbance at 600 nm (OD$_{600}$) = 0.1, and 200 μl was added to 96-well plates and grown at 37 °C with shaking in a TECAN plate reader. Growth was measured as an increase in OD$_{600}$, with values taken every 20 min up to 48 h. For *M. pneumoniae* growth curves, strains were inoculated in Hayflick medium in a T75-cm^2 flask and grown at 37 °C. After 3 d, cells were scraped from the flasks and resuspended in 1 ml of Hayflick medium. The cell suspension was then diluted 1:200 and 200 μl of this suspension was added to 96-well plates and incubated on static conditions at 37 °C in a TECAN plate reader. Growth was measured as an increase of the ratio between absorbance at 430 nm and 560 nm, with values at 430 nm and 560 nm taken every 2 h for 4 d.

Plasmids

All plasmids generated in this work were assembled following the Gibson method[63]. When required, IDT Incorporation performed gene synthesis. Oligonucleotides were synthesized by Sigma-Aldrich. Gene amplifications were carried out with Phusion DNA polymerase (Thermo Fisher Scientific). A description of the plasmids is available in Supplementary Table 3. The final sequence of all the plasmids was checked by Sanger sequencing (Eurofins Genomics).

Generation of *M. pneumoniae* mutant strains

The mutant strain Δ*mpn453* and CV2 (double mutant carrying deletions in both *mpn133* and *mpn372*) genes were constructed in previous work[62]. *M. pneumoniae* strains with genetic platforms were generated by transforming the CV2 and WT strains with vectors described in Supplementary Table 3 by electroporation. After pulsing, cells were selected in T75-cm^2 flasks containing 25 ml of plain Hayflick medium with selective antibiotics (tetracycline, 2 μg ml^{-1}, gentamicin, 100 μg ml^{-1}, or chloramphenicol, 20 μg ml^{-1}).

Protein quantification by MS

For the proteome samples of different mutant strains, *M. pneumoniae* strains were grown to the exponential phase of growth. After a medium sample of 2 ml was removed, cells were washed 3× with PBS and collected in 1 ml of PBS by scraping. Cell samples were centrifuged at 14,000*g* for 15 min and the pellet was resuspended in 50 μl of 6 M urea (in 200 mM ammonium bicarbonate). The medium samples were centrifuged at 14,000*g* and then passed over a 0.1-μm filter. The 800-μl sample was concentrated to 50 μl using 3K MWCO columns, and 75 μl of urea in 200 mM ammonium bicarbonate was added to a final concentration of 6 M urea. After 15 min of sonication, all samples were quantified using bicinchoninic acid and then processed for MS. Samples were analyzed by tandem MS combined with liquid chromatography. Briefly, in solution digestion samples were reduced with dithiothreitol (30 nmol, 1 h, 37 °C) and alkylated in the dark with iodoacetamide (60 nmol, 30 min, 25 °C). The resulting protein extract was first diluted 1:3 with 200 mM NH$_4$HCO$_3$ and

digested with 1 μg of LysC (Wako, catalog no. 129–02541) overnight at 37 °C and then diluted 1:2 and digested with 1 μg of trypsin (Promega, catalog no. V5113) for 8 h at 37 °C. The tryptic peptides were then first acidified and desalted with a MicroSpin C18 column (The Nest Group, Inc.). Samples were analyzed using an LTQ-Orbitrap Velos Pro mass spectrometer coupled to an EASY-nLC 1000 (Thermo Fisher Scientific). The sample was loaded on to the 2-cm Nano Trap column (inner diameter 100 μm, 5-μm C18 particles; Thermo Fisher Scientific) and separated by reversed-phase chromatography using a 25-cm column (inner diameter 75 μm, 1.9-μm C18 particles; Nikkyo Technos Co., Ltd.). Chromatographic gradients started at 93% buffer A and 7% buffer B with a flow rate of 250 nl min^{-1} for 5 min and gradually increased to 65% buffer A and 35% buffer B in 120 min. After each analysis, the column was washed for 15 min with 10% buffer A and 90% buffer B. Buffer A is 0.1% formic acid in water and buffer B 0.1% formic acid in acetonitrile. The mass spectrometer was operated in positive ionization mode with nanospray voltage set at 2.1 kV and source temperature at 300 °C. Before the analysis, we performed external calibration of the Fourier transform with Ultramark 1621 and internal calibration with the ion signal of the poly(siloxane) background (*m/z* 445.1200). For the MS scans, the data-dependent acquisition (DDA) mode was set at a resolution of 60,000, *m/z* range 350–2,000 and detected in the Orbitrap (automatic gain control (AGC) = 1×10^6 and dynamic exclusion of 60 s). The top 20 most intense ions were selected for collision-induced dissociation fragmentation with normalized collision energy of 35% in each cycle of DDA analysis. For the injection, we selected AGC to 1×10^4, 2.0-*m/z* isolation window, 10 ms of activation time and 100 ms of maximum injection time. Xcalibur software v.2.2 was used for data acquisition. To eliminate sample residues and ensure the stability of the equipment, we analyzed digested bovine serum albumin (New England Biolabs) between samples[66]. Proteome Discoverer (Thermo Fisher Scientific) software and Mascot[67] and search engine (Matrix Science) were used for the analysis of the acquired spectra. The data were searched against an *M. pneumoniae* database plus a list of common contaminants[68] (87,070 entries) and all the corresponding decoy entries. A precursor ion mass tolerance of 7 p.p.m. was used for MS1 level for peptide identification, using trypsin as the enzyme and allowing up to three missed cleavages. For MS2 spectra, ion mass tolerance was established at 0.5. We used oxidation of the methionine and amino-terminal protein acetylation as variable modifications, and carbamidomethylation on cysteine as a fixed modification. The false discovery rate in peptide identification was set to a maximum of 5%.

The 'precursor ion area detector' node from Proteome Discoverer (v.2.0) was used for peptide quantification. The obtained values were used to calculate the protein top three areas with the unique peptide for protein ungrouped (Supplementary Table 4). The raw proteomics data have been deposited to the PRIDE[69] repository with the accession no. PXD037233.

In vitro biofilm degradation assay

M. pneumoniae was grown in a T25-cm^2 flask for 3 d with 5 ml of Hayflick medium without antibiotics and then the conditioned supernatant was filtered with 0.33-μm sterile syringe filters. *P. aeruginosa* strains were grown overnight in Erlenmeyer flasks (20 μl stock in 20 ml of TSB) at 37 °C on shaking at 600 r.p.m., and then diluted to an OD$_{600}$ of 0.15 in TSB. Diluted *Pseudomonas* culture (100 μl) was then added in triplicate to sterile 96-well, polystyrene microtiter plates. Cells were incubated statically at 37 °C for 24 h to allow for biofilm formation. Biofilms were washed with PBS the following day to remove nonadherent cells and TSB medium. Treatments of 50–100 μl of *M. pneumoniae*-conditioned filtered medium were added to the wells (using triplicates or more) and plates were incubated at 37 °C for 4 h. After incubation, wells were washed with PBS, stained with 150 μl of 0.1% (w:v in water) Crystal Violet

(Sigma-Aldrich) for 10 min, or with 150 µl of 0.1% (w:v in 3% acetic acid) Alcian Blue (Sigma-Aldrich), and washed 3× with PBS. The dye was solubilized by addition of 100 µl of 95% (v:v) ethanol and incubated for 10 min. Absorbance was measured at 595 nm (for Crystal Violet) or 620 nm (for Alcian Blue) using a TECAN plate reader.

To measure the impact of *M. pneumoniae* supernatants on the number of PAO1 cells, biofilms were formed in 96-well plate and treated as described above. After incubation, supernatants were removed and the attached cells were recovered in 200 µl of PBS, serially diluted, seeded on *Pseudomonas* agar plates and incubated at 37 °C for 24 h. The colony-forming units were counted in two independent experiments with three technical triplicates each.

In vitro antimicrobial activity test

The antimicrobial activities of the supernatant of *M. pneumoniae* strains expressing pyocins were tested in a growth curve. *M. pneumoniae* was grown in a T25-cm^2 flask to confluence (3–4 d at 37 °C, 5% CO_2) with 5 ml of Hayflick medium without antibiotics, and then the supernatant medium was filtered with 0.33-µm sterile syringe filters. *P. aeruginosa* strains were grown overnight in Erlenmeyer flasks (20 µl of stock in 20 ml of TSB) at 37 °C with shaking and then diluted to an OD_{600} of 0.1 in TSB. Diluted *Pseudomonas* culture (180 µl) was mixed with 20 µl of filtered *M. pneumoniae* supernatant into sterile, 96-well, polystyrene microtiter plates. All conditions were tested at least in triplicate. Plates were incubated in a TECAN reader at 37 °C with shaking and the OD_{600} was measured every 20 min.

Mice experiments

Ethics. The animals used in all the studies were CD1 mice (female and male, weight 18–22 g and aged 4–6 weeks), purchased from Charles River Laboratories, and specific pathogen free. Group animal size were computed with G*Power software. The number of animals used in each experiment is specified in the figure legends.

The experiments, aimed to set up the routes of administration, the *M. pneumoniae* doses and the CV2 strain safety, were performed either at the Institute of Agrobiotechnology facilities (registration no. ES/31-2016-000002-CR-SU-US) or at the Barcelona Biomedical Research Parc (PRBB) facilities (registration no. B9900073). All the procedures involving animals were legislated for by the European Directive 86/609/EEC and the National law (Real Decreto 53/2013), in accordance with the FELASA and ARRIVE guidelines and the agreement of the Universidad Pública de Navarra (UPNa), the PRBB Animal Experimentation Committee (Comité de Ética, Experimentación Animal y Bioseguridad) and the local government authorization. The experiments aimed at studying the efficacy in vivo were performed in the UK under the Home Office Licence PA67E0BAA with local ethical committee clearance (Animal Welfare and Ethical Review Body). All the experiments were performed in dedicated Biohazard 2 facilities (this site holds a Certificate of Designation). On receipt at the facility, animals were housed in sterilized, individually ventilated cages connected to HEPA (high-efficiency particulate absorbing)-filtered sterile air and allowed to acclimatize for at least 7 d. Mice always had free access to food and water (sterile) and aspen chip bedding. The room temperature was 22 °C ± 1 °C, with a relative humidity of 60% and maximum background noise of 56 dB. Mice were exposed to 12:12 h light:dark cycles. Mice were monitored at least once daily for their clinical condition and assessed for their clinical score. The clinical score was given as follows: 1 = no deterioration in clinical condition, may include slight piloerection, normal activity; 2 = slight piloerection, slightly hunched, dehydrated, weight loss <20%; 3 = piloerection, moderate intermittent hunching, dehydrated, weight loss <20%, orbital tightening/eye discharge, irregular breathing, slightly reduced mobility, slightly reduced activity, sides pinched in, slight drop in temperature: animal can continue on study but should be monitored closely; 4 = piloerection, moderate persistent hunching for up to 1 h, dehydrated, weight loss >20%, orbital

tightening/eye discharge, reduced breathing rate, increased breathing depth, subdued, reduced activity, cold to touch, pale in color: animal has reached moderate endpoint and should be euthanized.

Inoculations. To prepare cell suspension for the inoculations, *M. pneumoniae* strains were grown in a T75 culture flask (Sarstedt) with Hayflick-ampicillin 100 µg ml^{-1} (H-Amp$_{100}$) broth (37 °C, 3–4 d, 5% CO_2). After washing, cells were scraped with PBS and passed through a syringe (25G). Appropriate suspensions (c.f.u. µl^{-1} indicated in each experiment) were prepared and an aliquot was plated on H-Amp$_{100}$ agar to assess bacterial counts. *P. aeruginosa* PAO1 was grown overnight in TSB broth at 37 °C on shaking and diluted with PBS to an optimal concentration. For the efficacy studies, mice were rendered neutropenic with two subcutaneous injections of cyclophosphamide: 150 mg kg^{-1} at 4 d before PAO1 infection and 100 mg kg^{-1} at 1 d before PAO1 infection. Before inoculation with *M. pneumoniae* or PAO1, mice were anesthetized with isoflurane 2% (ISOFLO, Covegan). Intratracheal inoculation was performed by introducing 100 µl of cell suspension through a sterile 20G (1.1-mm diameter) Vialon intravenous catheter (Becton-Dickinson) inserted into the trachea. Intranasal inoculation was performed by pipetting 20 µl of cell suspension into both nostrils (total volume was 40 µl). Mice were then released into their cages and monitored until they regained consciousness.

Mouse sampling. Mice were necropsied at 2, 14 and 45 d.p.i. Lungs were collected and processed for histological studies according to Morton and Snider[65]. Briefly, lungs were insufflated with 10% formalin through the trachea in situ and then removed and fixed in formalin for 24 h for histological analysis.

For RNA extraction, lungs were sectioned and immediately frozen in liquid nitrogen and stored at −80 °C until use. When required, BALF samples were obtained by intratracheal perfusion and harvesting of 0.7 ml of PBS pe rmouse, with a sterile 20G Vialon catheter.

For bacteriological analysis, lung and BALF samples were serially tenfold diluted in sterile PBS and plated by triplicate to determine the number of viable bacteria on Hayflick-ampicillin agar (for *M. pneumoniae*) or *Pseudomonas* agar (Oxoid, for *P. aeruginosa*). Plates were incubated at 37 °C for 14 d (for *M. pneumoniae*) or 16–24 h (for *P. aeruginosa*), and then colonies were counted using a Leica Zoom 2000 plate microscope at ×10 magnification.

Lung RNA extraction and RT−qPCR analysis

Lungs previously stored at −80 °C were homogenized using Ultra-Turrax (IKA) and total RNA was isolated using RNeasy Mini Kit (QIAGEN), following the manufacturer's instructions. RNA concentrations were measured spectrophotometrically using Nanodrop One (Thermo Fisher Scientific), and sample RNA integrity was confirmed by 1% agarose gel electrophoresis. RNA samples with the ratio of absorbance at 260 nm:280 nm of 1.8–2.1 were used. Complementary DNA from whole lung cells was synthesized from total RNA (1 µg) using SuperScript II Reverse Transcriptase reagents (Invitrogen). PCR amplification was performed using SYBR Premix Ex Taq II (Tli RNaseH Plus; Takara) and fluorescence was analyzed with AriaMx Real-Time PCR System (Agilent Technologies). The comparative threshold cycle (C_t) method[70] was used to obtain relative quantities of messenger RNAs that were normalized using *gapdh* as an endogenous control. Primer sequences for the genes *tnf*, *il1b*, *il6*, *il12a*, *il23a*, *ifng*, *ccl2*, *ccl3*, *cxcl1* and *gapdh* are shown in Supplementary Table 7.

Histopathological analysis of lung samples

After necropsy, lung samples were insufflated with formalin, fixed for at least 24 h, trimmed and then automatically processed in ethanol series and xylene substitute (Citadel 2000 Tissue Processor, Thermo Fisher Scientific). Thereafter, tissues were embedded in paraffin (HistoStar Embedding Workstation, Thermo Fisher Scientific), sectioned at 4 µm

(Finesse ME + Microtome, Thermo Fisher Scientific), stained with haematoxylin and eosin (H&E) (Gemini AS Automated Slide Stainer, Thermo Fisher Scientific) and mounted on glass slides (CTM6 Coverslipper Thermo Fisher Scientific). For light microscopy analysis, histological images were obtained using a digital camera (MC170 HD, Leica) connected to an optical microscope (DM2000, Leica) using a commercial software (Leica Application Suite, v.4.6.0). Sections were examined blind as sets by a trained veterinary pathologist and lesions were scored based on five parameters: (A) peribronchial/peribronchiolar inflammatory infiltrate affectation (0, none; 1, <25%; 2, 25–75%, 3, >75%); (B) peribronchial/peribronchiolar inflammatory infiltrate intensity (0, none; 1, incomplete infiltration; 2, complete infiltration, <5 cells thick; 3, complete infiltration, ≥5 cells thick); (C) bronchial/bronchiolar luminal exudate intensity (0, none; 1, <25% of lumen occlusion; 2, >25% of lumen occlusion); (D) perivascular inflammatory infiltrate affectation (0, none; 1, <10%; 2, 10–50%; 3, >50%); and (E) interstitial pneumonia intensity (0, none; 3, multifocal foci of interstitial pneumonia; 5, multifocal-coalescing foci to diffuse interstitial pneumonia). According to previous studies[62,63], a final score (0–26) was obtained with the formula A + (3 × (B + C)) + D + E.

Dispersal of ETT biofilms from patients

ETTs from patients receiving MV were collected from September 2015 to December 2017. They were selected from patients with a positive respiratory culture for *P. aeruginosa* during intubation, ventilated over 11 (6.00–16.50) d and in the confirmed presence of *P. aeruginosa* in ETTs (2.57 (2.20–4.81) $\log_{10}$(c.f.u. ml^{-1})) at extubation of the patient. ETTs were frozen until analysis, in a collection carried out in compliance with the Declaration of Helsinki (current version, Fortaleza, Brazil, October 2013). The collection was approved by the institution's internal review board (Ethical Committee for Research in Medicines, Hospital Clinic of Barcelona, Spain), with the registry no. R190311-203;HCB/2019/026. Afterwards, ETTs were slowly unfrozen to room temperature and sliced into the following sections with different treatments: control (Hayflick medium alone without treatment); CV2_HA_PL1 (-1 × 10^8 log(c.f.u. ml^{-1})), C/T (Zerbaxa 1 g per 0.5 g powder, 5 µg ml^{-1}) and CV2_HA_P1 + C/T. The CV2_HA_P1 inoculum contained 7.32 (8.26–9.20) log(c.f.u. ml^{-1}) (Fig. 4a)[71].

Each ETT section and treatment condition were adjusted to a final volume of 1,600 µl with Hayflick medium and incubated at 37 °C for 24 h. Before diluting (−1 to −5(log$_{10}$)) and culturing on MacConkey and blood agar (Becton-Dickinson GmbH), samples were sonicated for 5 min at 40 kHz in ultrasound-cleaning equipment (Branson 3510 E-MT; Bransonic) as previously published[71]. *P. aeruginosa* counts in each treatment were reported in log$_{10}$(c.f.u. ml^{-1}). A complete antibiogram (amikacin, colistin, piperacillin/tazobactam, aztreonam, tobramycin, ceftazidime, meropenem or imipenem) was performed for each *P. aeruginosa* strain using the Kirby–Bauer method, with the *P. aeruginosa* American Type Culture Collection 27853 strain as a control. The interpretation of results was carried out according to the European Committee on Antimicrobial Susceptibility Testing. *P. aeruginosa* was considered to be multidrug resistant when nonsusceptible to three or more families of antipseudomonal antimicrobials[72]. In addition, molecular epidemiology was analyzed by multilocus sequence typing (https://pubmlst.org/paeruginosa). Phylogenetic analysis was carried out using the eBURST algorithm (http://www.phyloviz.net/goeburst).

Statistical analysis

Categorical variables were reported as number (%), whereas continuous variables were reported as mean ± s.d. or median (interquartile range (IQR)), if the distribution was normal or non-normal, respectively. Continuous variables between groups were compared using the one-way analysis of variance (ANOVA) followed by a post-hoc, pairwise Tukey's honestly significant difference (HSD) or a Kruskal–Wallis test, as appropriate. Paired samples were compared using the paired Student's

t-test or nonparametric Wilcoxon's signed-rank test when appropriate. Spearman's correlation analyses were performed to determine associations between continuous variables. In all the cases, $P ≤ 0.05$ was considered to be statistically significant and the exact P value is specified in figure legends when possible. Data were analyzed using StatsDirect software (v.3.1.8) or GraphPad Prism (v.8.0.1).

Reporting summary

Further information on research design is available in the Nature Portfolio Reporting Summary linked to this article.

Data availability

The MS dataset has been submitted to the public data repository PRIDE (PRoteomics IDEntifications database) with the following accession no.: PXD037233.

References

66. Olivella, R. et al. QCloud2: an improved Cloud-based quality-control system for mass-spectrometry-based proteomics laboratories. *J. Proteome Res.* **20**, 2010–2013 (2021).
67. Perkins, D. N., Pappin, D. J., Creasy, D. M. & Cottrell, J. S. Probability-based protein identification by searching sequence databases using mass spectrometry data. *Electrophoresis* **20**, 3551–3567 (1999).
68. Beer, L. A., Liu, P., Ky, B., Barnhart, K. T. & Speicher, D. W. In *Serum/Plasma Proteomics* Vol. 1619 (eds Greening, D. W. & Simpson, R. J.) 339–352 (Springer, 2017).
69. Vizcaíno, J. A. et al. 2016 update of the PRIDE database and its related tools. *Nucleic Acids Res.* **44**, 11033 (2016).
70. Livak, K. J. & Schmittgen, T. D. Analysis of relative gene expression data using real-time quantitative PCR and the 2$^{-\Delta\Delta CT}$ method. *Methods* **25**, 402–408 (2001).
71. Fernández-Barat, L. et al. Linezolid limits burden of methicillin-resistant *Staphylococcus aureus* in biofilm of tracheal tubes. *Crit. Care Med.* **40**, 2385–2389 (2012).
72. Magiorakos, A.-P. et al. Multidrug-resistant, extensively drug-resistant and pandrug-resistant bacteria: an international expert proposal for interim standard definitions for acquired resistance. *Clin. Microbiol. Infect.* **18**, 268–281 (2012).

Author contributions

R.M. and I.R.-A. designed and performed experiments, analyzed data and wrote the paper. L.F.-B., C.P.-L. and V.G. designed and performed experiments. A.R.-M. and A.M. analyzed data. A.T. and M.J.-G. gave technical support and conceptual advice. L.S. and M.L.-S. designed

experiments, analyzed data, gave technical support and conceptual advice, wrote the paper and led the project.

Competing interests

Additional information
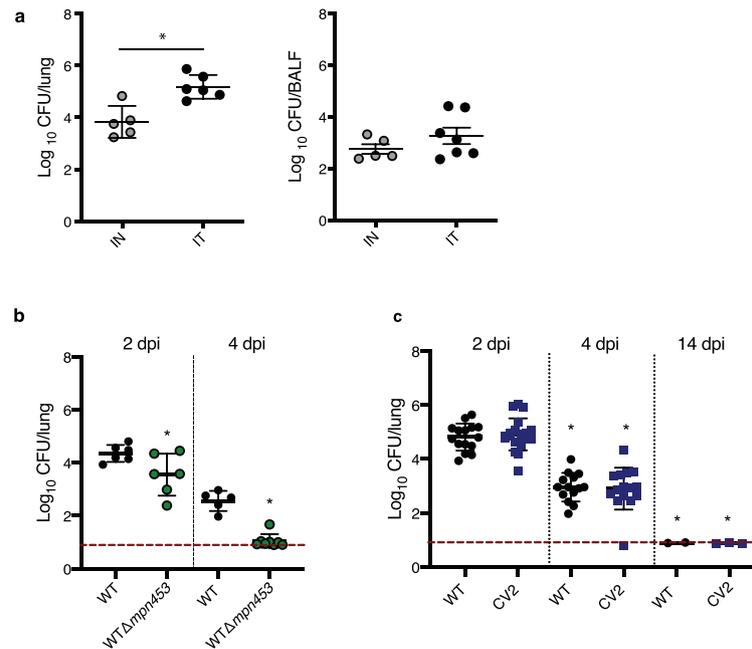
Extended Data Fig. 1 | Delivery route and lung infection dynamic of *M. pneumoniae* WT and mutant strains generated in this study. a, CFUs per lung (left) or BALF (right) in CD1 mice infected using the same dose (-1×10^7 CFU/mice), by intranasal (IN, 20 μl. Five animals) or intratracheal (IT, 100 μl. Six animals) administration. Mice were euthanized at 2 days post-infection (dpi) to determine bacterial load in lungs (left panel, log$_{10}$ CFU/lung) and in BALF (right panel, log$_{10}$ CFU/lung or BALF). Data are expressed as mean ± standard deviation (SD). Statistical comparison was performed using two-sided t-test. *P = 0.032. b, The WTΔ*mpn453* mutant strain is eliminated faster than the WT strain. Two-sided

t-test was used (*P = 0.04 and P = 0.02). Data are expressed as mean ± standard deviation (SD). c, Lung infection dynamics of *M. pneumoniae* WT and CV2 chassis strains. Bacterial counts were obtained at 2 dpi (n = 15), 4 dpi (n = 15) or 14 dpi (n = 3) for both strains. Data are shown as means values ± SD of log$_{10}$ CFU/lung. Statistical comparisons were performed using two-sided t-test. *P < 0.05. Red line, experimental detection limit (log$_{10}$ CFU/lung = 0.7–0.9). Infections were performed in all cases in groups of at least five mice per strain and/or time point ($n ≥ 5$).
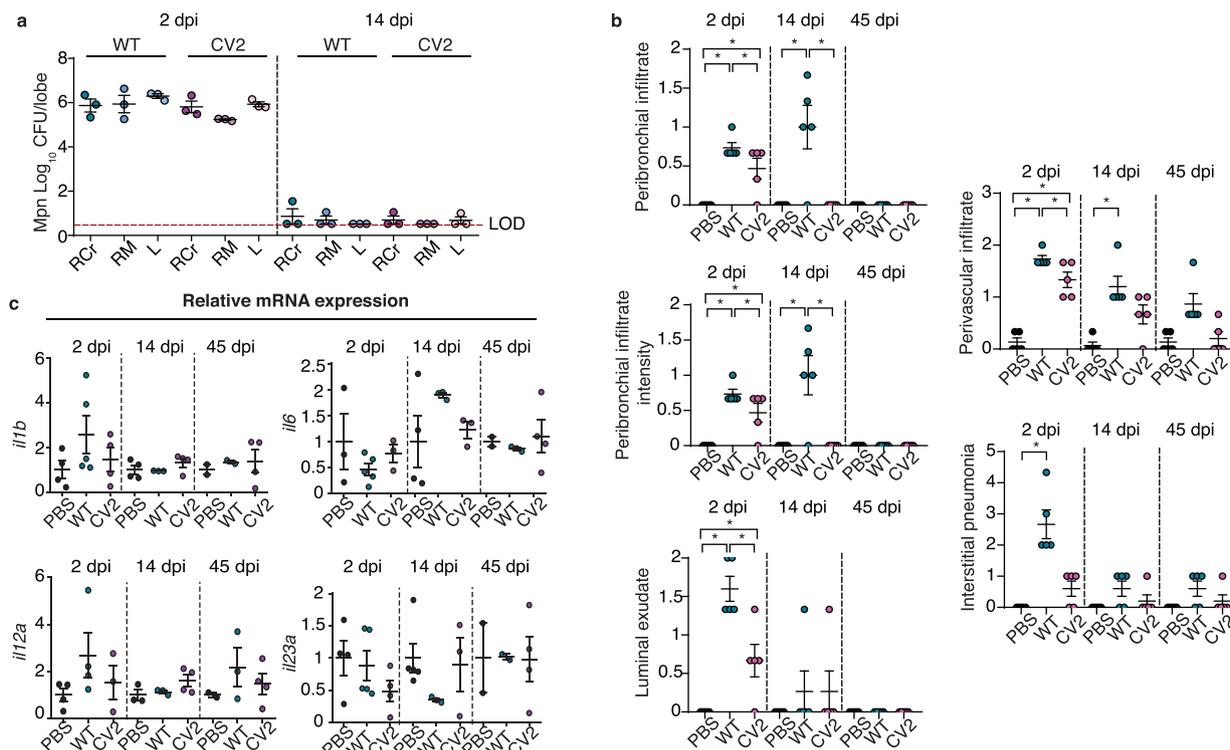
Extended Data Fig. 2 | Analysis of the lungs of the animals inoculated with WT or CV2. a, CFUs of the strains WT or CV2, at 2 or 14 days post-inoculation (dpi), found in three major lung lobes (RCr, right cranial; RM, right medium; and L, left. N = 3 animals per group). LOD = limit of detection. Data are expressed as mean ± SD. b, Scoring of the individual parameters analyzed in the histopathologic study of lung sections from mice inoculated with PBS, WT or CV2, analysed at 2, 14 or 45 dpi. See Methods for a detailed description of the histopathological scoring system used. Data are presented as mean values

± SD. Statistical comparisons were performed with One-way ANOVA + Tukey's multiple comparison test; *P < 0.05. c, Pulmonary inflammatory response to *M pneumoniae* is independent of *il1b*, *il6*, *il-12a* or *il23a*. Gene expression was analysed by RT-qPCR at 2-, 4- and 45 dpi from lungs inoculated with PBS or with WT or CV2 *M. pneumoniae* strains. Data are presented as mean values ± SD. Each animal is represented as an individual plot (At 2 dpi: PBS n = 4; CV2 n = 5; CV2_HA_P1 n = 4; at 14 dpi, PBS n = 5; CV2 n = 4; CV2_HA_P1 n = 4 M; at 45 dpi: PBS n = 2; CV2 n = 4; CV2_HA_P1 n = 4).
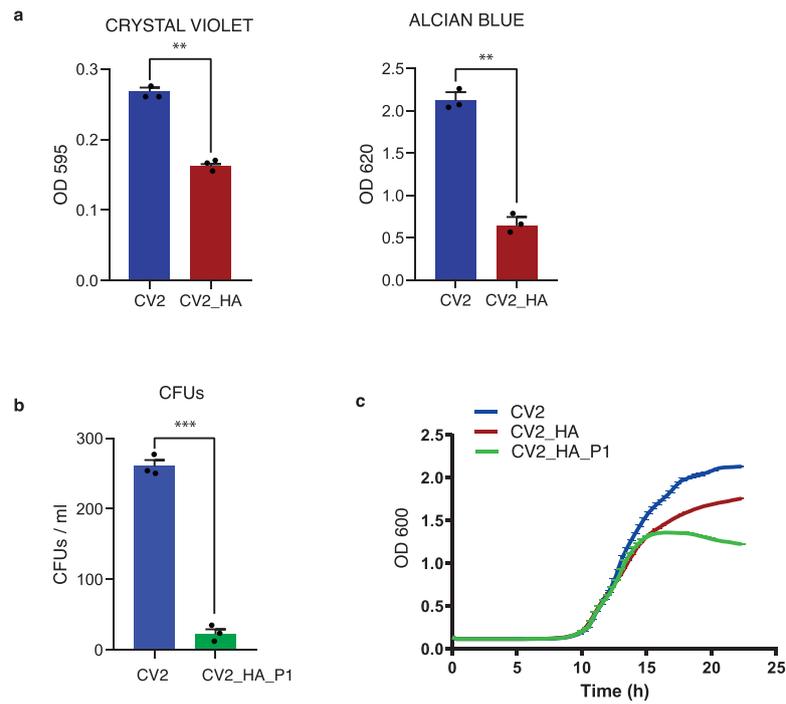
Extended Data Fig. 3 | Effect of CV2_HA on *P. aeruginosa* PAO1 biofilm and growth. a, Dispersal activity of CV2_HA on PAO1 biofilm, quantified after staining with crystal violet or Alcian blue. Pseudomonas biofilms were generated by seeding in 96-well plates and incubating at 37 °C for 24 h. Biofilms were then treated at 37 °C for 4 h with *M. pneumoniae* CV2_HA supernatants, to allow the activity of the dispersal enzymes. The remaining biofilm was stained with crystal violet or Alcian blue and quantified with a plate reader at the indicated absorbances (OD 595 or OD 620). Three independent experiments performed. Data are presented as mean values ± SD. **$P = 0.009$ and $P = 0.007$, two-sided *t*-test. b. Activity of CV2_HA_P1 on PAO1 biofilm, quantified as CFUs/ml. Pseudomonas biofilms were generated by seeding in 96-well plates and incubating at 37 °C for 24 h. Biofilms were then treated at 37 °C for 4 h with the indicated supernatants, and then the remaining biofilm was resuspended in PBS and seeded on Pseudomonas agar plates. Three independent experiments performed. Data are presented as mean values ± SD. ***$P < 0.001$, two-sided *t*-test. c, Growth curves of *P. aeruginosa* strain PAO1 in presence of supernatant from CV2, CV2_HA or CV2_HA_P1. Results from triplicate samples are shown. Data are presented as mean values ± SD. Details of the assay are given in the Methods.
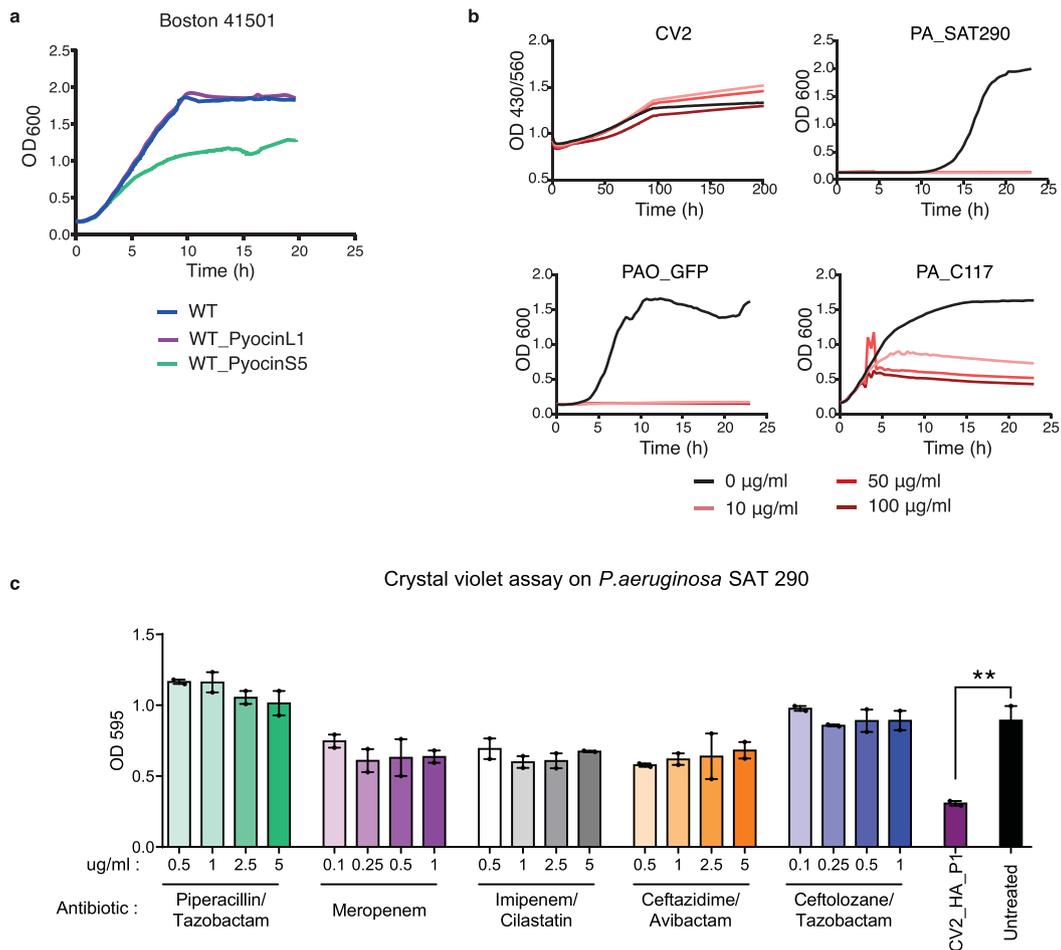
Extended Data Fig. 4 | Study of effect of antibiotics on growth curves and biofilms formation. a, Effect of treatment with the WT *M. pneumoniae* strain expressing pyocin L1 or pyocin S5 on the growth of the *P. aeruginosa* Boston 41501 strain. b, Growth curves of CV2 and different *P. aeruginosa* strains (SAT290, PAO1 or C117) in the presence of different doses of the antibiotic combination piperacillin/tazobactam. Growth was measured by absorbance determination at OD 430/560 or OD 600. c, Crystal violet assay measuring *P. aeruginosa* SAT290 biofilm degradation using different antibiotics at different concentrations. Two independent experiments performed. Data are presented as mean values ± SD. **P = 0.004, two-sided t-test. No significant effects on biofilm degradation were observed as compared to the untreated control. Details of the assays are given in the Methods.
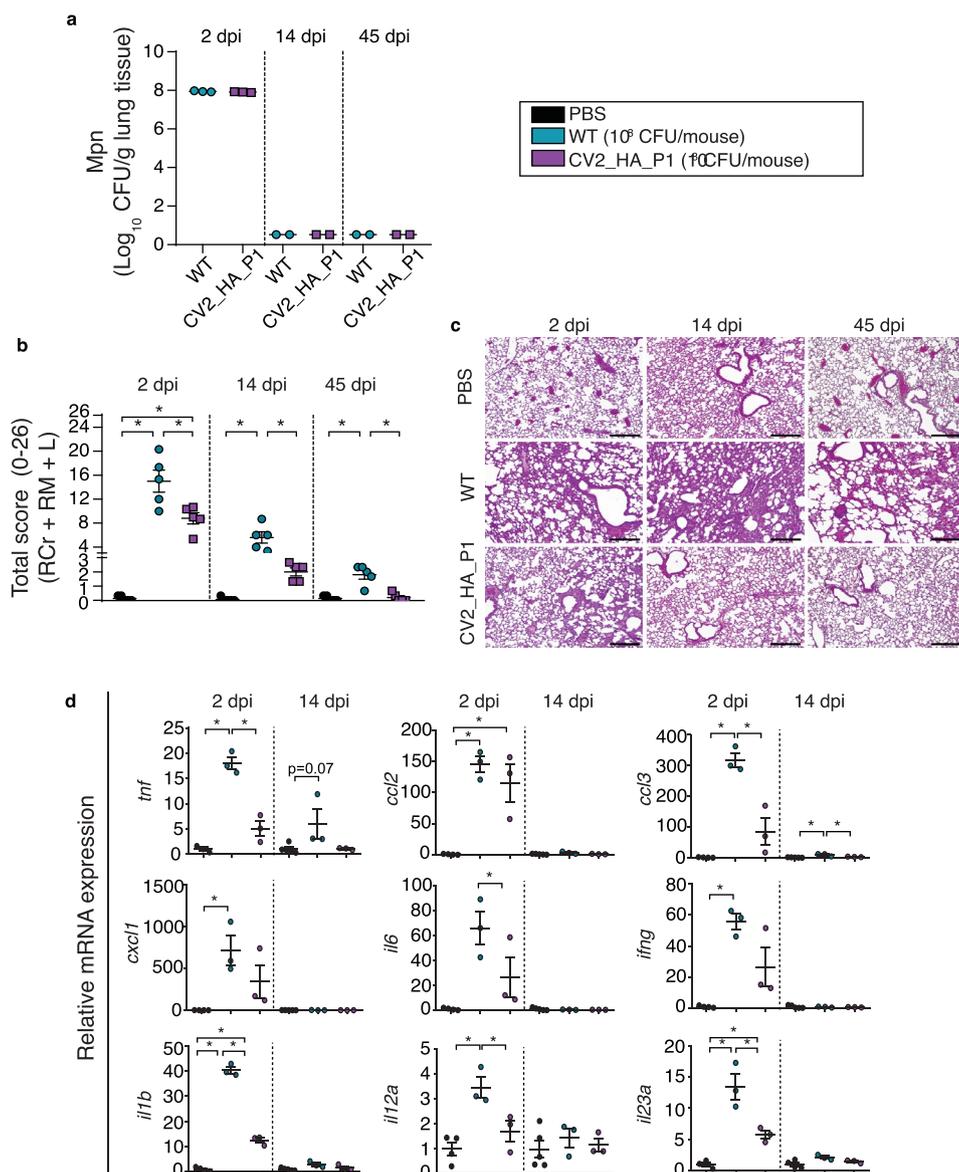
Extended Data Fig. 5 | Tissue lesions and inflammatory response of lungs infected with *M. pneumoniae* WT and CV2_HA_P1 strain at 10⁸ CFUs. CD1 mice were inoculated intratracheally with *M. pneumoniae* CV2_HA_P1, WT or PBS (as control), and lungs were analysed at 2-, 14- and 45 dpi. a, CFUs of the strains WT or CV2_HA_P1, at 2, 14 or 45 days post-inoculation (dpi) recovered in lungs (n = 3, 2 and 2, respectively). b, Lung lesions evaluation, expressed as the total final score of the histological analysis performed on three major lobes, with five animals per group (each data point is the average of the total score of the Right Cranial, Right Middle and Left of each animal). Data are presented as mean values of each group ± SD. *P < 0.05; One-way ANOVA + Tukey's multiple comparison test. For detailed description of the scoring system used in the histopathological analysis, see Methods. c, Representative H&E-stained lung sections (100·, scale bar 100 μm) from the left lobe, obtained using a digital camera (MC170 HD, Leica) connected to an optical microscope (DM2000, Leica) using a commercial software (Leica Application Suite, version 4.6.0). d, Gene expression of inflammatory markers, assessed by RT-qPCR. Data are shown as mean ± SD of 2^{-ΔΔCt}. Each animal is indicated as an individual plot. Each animal is represented as an individual plot (PBS, n = 4; CV2, n = 3; CV2_HA_P1, n = 3). *P < 0.05, One-way ANOVA + Tukey's multiple comparison test.
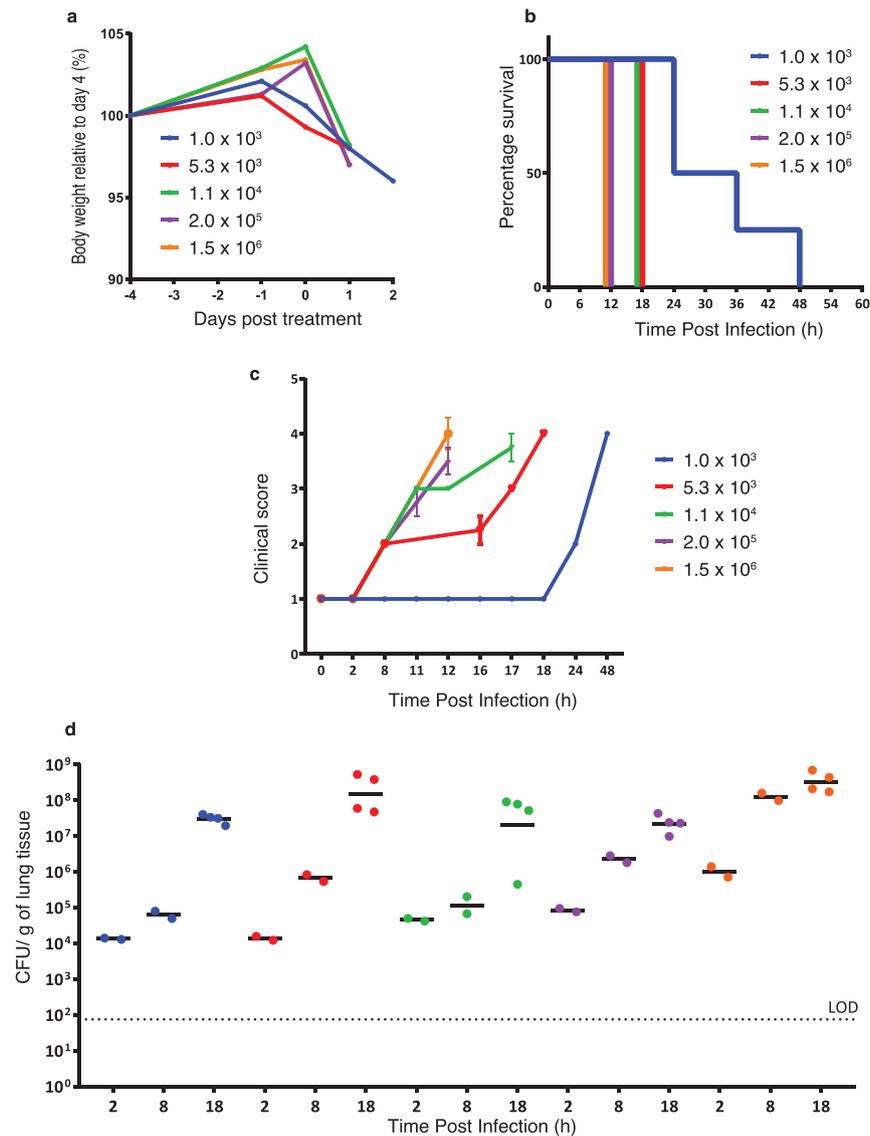
Extended Data Fig. 6 | Set up of acute model of *P. aeruginosa* infection. CD1 mice were IT infected with different amounts of P. aeruginosa PAO1 (1.0×10^3, 5.3×10^3, 1.1×10^4, 2.0×10^5 or 1.5×10^6 CFU/mouse). a, Evaluation of body weight of mice infected with different doses of *P. aeruginosa* PAO1. b, Endpoints at which mice were euthanized by pentobarbitone overdose. c, Clinical score (see Methods) of the mice infected with different doses of *P. aeruginosa* PAO1 (Five animals per groups. Data are presented as mean values ± SD.). d, Number of CFUs recovered from the lung of mice after inoculation with different doses of PAO1 at different time points post-inoculation (2, 8 or 18 hpi. N = two or four animals per group, as indicated by the data points). LOD = Limit of detection.
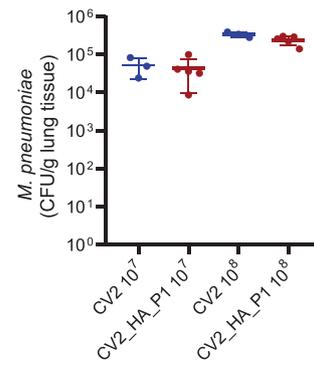
Extended Data Fig. 7 | *M. pneumoniae* CFUs detected in lungs of animals of the efficacy assays. Number of CFUs of *M. pneumoniae* strains CV2 and CV2_HA_P1 strains (inoculated at 1×10^7 or 1×10^8 CFU/mouse) recovered from the lung at 24 hpi. Animals (n = 3 for CV2 controls, and n = 5 for CV2_HA_P1 group) were sacrificed and the lungs were homogenized and serial diluted on Hayflick-agar plates. Data are presented as mean values ± SD.
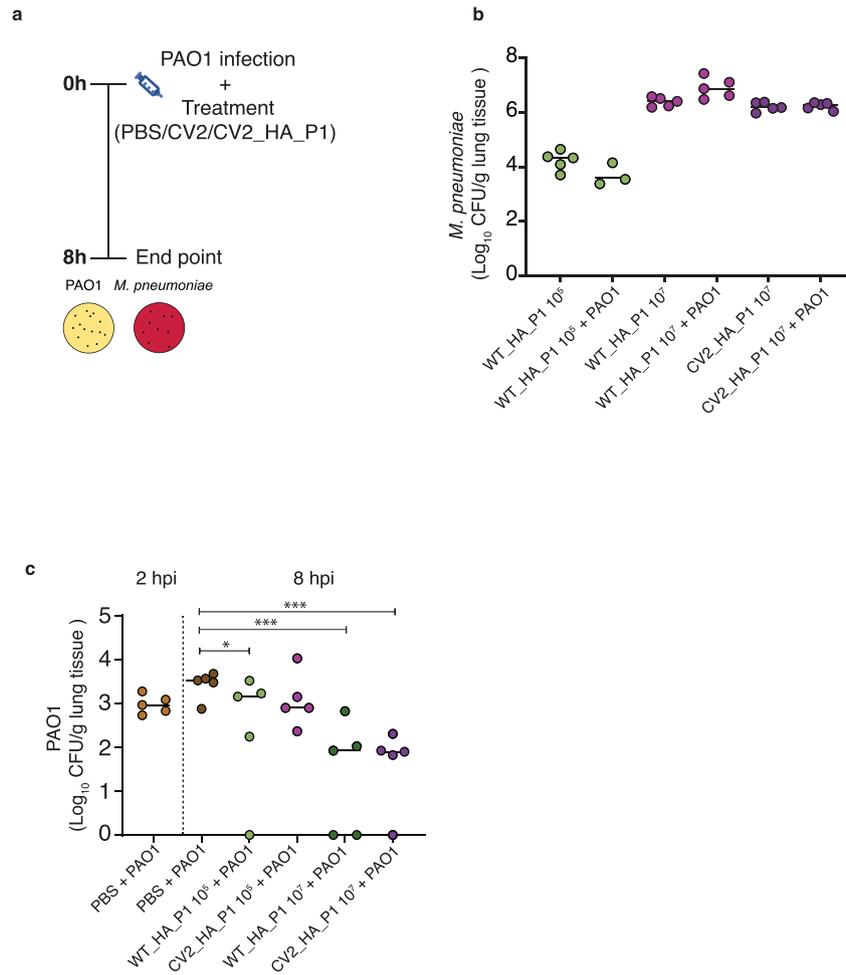
Extended Data Fig. 8 | Preventive effect of CV2_HA_P1 on pneumonia induced by PAO1. a, Schematic representation of the experimental design. Two amounts (1×10^5 or 1×10^7 CFU) of different *M. pneumoniae* strains, alone or in combination with *P. aeruginosa* PAO1 cells, were inoculated intratracheally in the animals (five animals per group). After 8 h, mice were sacrificed, and lungs were homogenized and seeded on Hayflick agar plates to quantify the CFU of *M. pneumoniae* strains (in b) or seeded on Pseudomonas agar to quantify PAO1 (in c). *$P < 0.05$, ***$P < 0.001$; P values of Kruskal–Wallis *H* test compared to the control at 8 h are indicated.

Corresponding author(s): Maria Lluch-Senar & Luís Serrano

Last updated by author(s): Sep 30, 2022

Reporting Summary

Nature Research wishes to improve the reproducibility of the work that we publish. This form provides structure for consistency and transparency in reporting. For further information on Nature Research policies, see our Editorial Policies and the Editorial Policy Checklist.

Statistics

For all statistical analyses, confirm that the following items are present in the figure legend, table legend, main text, or Methods section.

n/a	Confirmed	
☐	☒	The exact sample size (n) for each experimental group/condition, given as a discrete number and unit of measurement
☐	☒	A statement on whether measurements were taken from distinct samples or whether the same sample was measured repeatedly
☐	☒	The statistical test(s) used AND whether they are one- or two-sided *Only common tests should be described solely by name; describe more complex techniques in the Methods section.*
☐	☒	A description of all covariates tested
☐	☒	A description of any assumptions or corrections, such as tests of normality and adjustment for multiple comparisons
☐	☒	A full description of the statistical parameters including central tendency (e.g. means) or other basic estimates (e.g. regression coefficient) AND variation (e.g. standard deviation) or associated estimates of uncertainty (e.g. confidence intervals)
☐	☒	For null hypothesis testing, the test statistic (e.g. F, t, r) with confidence intervals, effect sizes, degrees of freedom and P value noted *Give P values as exact values whenever suitable.*
☒	☐	For Bayesian analysis, information on the choice of priors and Markov chain Monte Carlo settings
☐	☒	For hierarchical and complex designs, identification of the appropriate level for tests and full reporting of outcomes
☐	☒	Estimates of effect sizes (e.g. Cohen's d, Pearson's r), indicating how they were calculated

Our web collection on statistics for biologists contains articles on many of the points above.

Software and code

Policy information about availability of computer code

Data collection	No software was used
Data analysis	goeBURST algorithm, G*Power software (3.1), StatsDirect software (3.1.8) or GraphPad Prism (8.0.1)

For manuscripts utilizing custom algorithms or software that are central to the research but not yet described in published literature, software must be made available to editors and reviewers. We strongly encourage code deposition in a community repository (e.g. GitHub). See the Nature Research guidelines for submitting code & software for further information.

Data

Policy information about availability of data

All manuscripts must include a data availability statement. This statement should provide the following information, where applicable:
- Accession codes, unique identifiers, or web links for publicly available datasets
- A list of figures that have associated raw data
- A description of any restrictions on data availability

The authors declare that the data supporting the findings of this study are available within the paper.

Field-specific reporting

Please select the one below that is the best fit for your research. If you are not sure, read the appropriate sections before making your selection.

☒ Life sciences   ☐ Behavioural & social sciences   ☐ Ecological, evolutionary & environmental sciences

For a reference copy of the document with all sections, see nature.com/documents/nr-reporting-summary-flat.pdf

Life sciences study design

All studies must disclose on these points even when the disclosure is negative.

Sample size	Sample size was calculated using G*power software with the following parameter: error α:0.05; potency 1-β :0.8, values for parameter "final score of pulmonary lesions" based in previous experiment (average ±SD) 12.1±6 y 5.8±2.5, obtaining as a output n=5 mice per group.
Data exclusions	In the ex-vivo assays with sections of endotracheal tubes, one control sample was discarded because no P. aeruginosa counts could be obtained due to overgrowth of Proteus species.
Replication	All the in vitro assays were carried out using al least triplicate samples; all the assays were reproduced at least three independent times. In vivo assays with mice were performed with at least 6 animals in each experimental group, and all attempts at replication were successful. For any other epxeriments, independent experiments with triplicate samples were always performed.
Randomization	All the mice in the in vivo are commercial inbred strains assay, carrying the same genetic background. Hence, the animals were allocated randomly in each group. In the assays with ex-vivo endotracheal tubes, section of each tube were allocated randomly into experimental groups.
Blinding	The analysis of the ex-vivo samples (i.e. histopathology analysis) was analysed by a pathologist that did not know the ID of the samples. For experiments other than histopathology analysis, the investigators were also blinded to group allocation during data collection and/or analysis (i.e. animal health scoring during survival curves, counting of bacterial CFUs on plates). No blinding was required when objective data (i.e. absorbance values provided by plate reader, animals weights, Ct values from RT-qPCR) were analysed and plotted on graphs.

Reporting for specific materials, systems and methods

We require information from authors about some types of materials, experimental systems and methods used in many studies. Here, indicate whether each material, system or method listed is relevant to your study. If you are not sure if a list item applies to your research, read the appropriate section before selecting a response.

Materials & experimental systems

n/a	Involved in the study
☒	☐ Antibodies
☒	☐ Eukaryotic cell lines
☒	☐ Palaeontology and archaeology
☐	☒ Animals and other organisms
☐	☒ Human research participants
☒	☐ Clinical data
☒	☐ Dual use research of concern

Methods

n/a	Involved in the study
☒	☐ ChIP-seq
☒	☐ Flow cytometry
☒	☐ MRI-based neuroimaging

Animals and other organisms

Policy information about studies involving animals; ARRIVE guidelines recommended for reporting animal research

Laboratory animals	CD1 mice (female and male, 18–22 g, aged 4-6 weeks) were purchased from Charles River Laboratories (France)
Wild animals	The study did not involve wild animals
Field-collected samples	The study did not involve samples collected from the fied
Ethics oversight	- In vivo experiments produced by University of Navarra (Spain): Animal handling and procedures were in accordance with the current European (Directive 86/609/EEC) and National (Real Decreto 53/2013) legislations, following the FELASA and ARRIVE guidelines and with the approval of the Universidad Pública de Navarra (UPNa) Animal Experimentation Committee (Comité de Ética, Experimentación Animal y Bioseguridad) and the local Government authorization. - In vivo experiments produced by Evotec (UK): all in vivo animal studies were performed in the UK under the UK Home Office License PA67E0BAA, with the clearance of the local ethical committee Animal Welfare and Ethical Review Body.

Note that full information on the approval of the study protocol must also be provided in the manuscript.

Human research participants

Population characteristics	Endotracheal tubes were obtained from mechanically ventilated patients admitted to an Intensive Care Medicine Unit (Hospital Clinic of Barcelona) with ventilator associated pneumonia (VAP) due to P. aeruginosa
Recruitment	September 2015 to December 2017
Ethics oversight	Collection R190311-203; HCB/2019/0262. Approved by the Ethical Committee for Research in Medicines, Hospital Clinic of Barcelona, Spain.

Note that full information on the approval of the study protocol must also be provided in the manuscript.